ACS OMEGA

Open Access

http://pubs.acs.org/journal/acsodf

Article

Global Gene Expression Profiling and Bioinformatics Analysis Reveal Downregulated Biomarkers as Potential Indicators for Hepatocellular Carcinoma

Aktham Mestareehi*

Cite This: *ACS Omega* 2024, 9, 26075−26096

Read Online

ACCESS | Metrics & More | Article Recommendations | Supporting Information

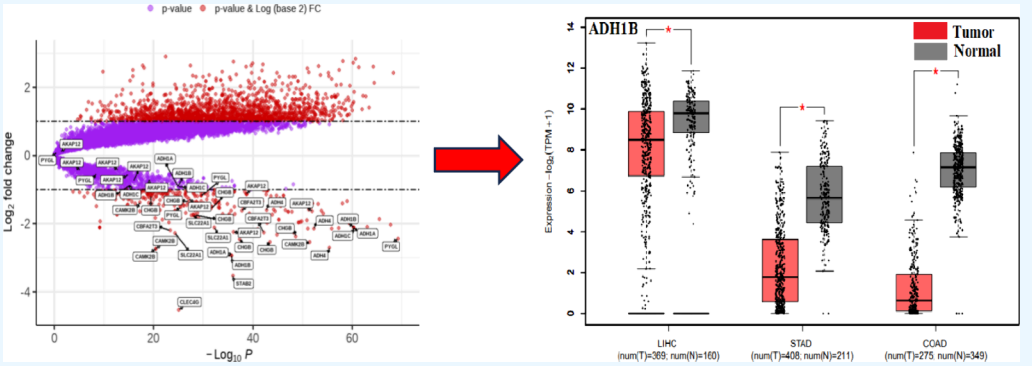

ABSTRACT: **Objective:** The study aimed to elucidate the significance of CLEC4G, CAMK2β, SLC22A1, CBFA2T3, and STAB2 in the prognosis of hepatocellular carcinoma (HCC) patients and their associated molecular biological characteristics. Additionally, the research sought to identify new potential biomarkers with therapeutic and diagnostic relevance for clinical applications. **Methods and Materials:** We utilized a publicly available high throughput phosphoproteomics and proteomics data set of HCC to focus on the analysis of 12 downregulated phosphoproteins in HCC. Our approach integrates bioinformatic analysis with pathway analysis, encompassing gene ontology (GO) analysis, Kyoto Encyclopedia of Genes and Genomes (KEGG) pathway analysis, and the construction of a protein−protein interaction (PPI) network. **Results:** In total, we quantified 11547 phosphorylation sites associated with 4043 phosphoproteins from a cohort of 159 HCC patients. Within this extensive data set, our specific focus was on 19 phosphorylation sites displaying significant downregulation ($\log_2$ FC ≤ -2 with p-values < 0.0001). Remarkably, our investigation revealed distinct pathways exhibiting differential regulation across multiple dimensions, including the genomic, transcriptomic, proteomic, and phosphoproteomic levels. These pathways encompass a wide range of critical cellular processes, including cellular component organization, cell cycle control, signaling pathways, transcriptional and translational control, and metabolism. Furthermore, our bioinformatics analysis unveiled noteworthy insights into the subcellular localizations, biological processes, and molecular functions associated with these proteins and phosphoproteins. Within the context of the PPI network, we identified 12 key genes CLEC4G, STAB2, ADH1A, ADH1B, CAMK2B, ADH4, CHGB, PYGL, ADH1C, AKAP12, CBFA2T3, and SLC22A1 as the top highly interconnected hub genes. **Conclusions:** The findings related to CLEC4G, ADH1B, SLC22A1, CAMK2β, CBFA2T3, and STAB2 indicate their reduced expression in HCC, which is associated with an unfavorable prognosis. Furthermore, the results of KEGG and GO pathway analyses suggest that these genes may impact liver cancer by engaging various targets and pathways, ultimately promoting the progression of hepatocellular carcinoma. These results underscore the significant potential of CLEC4G, ADH1B, SLC22A1, CAMK2β, CBFA2T3, and STAB2 as key contributors to HCC development and advancement. This insight holds promise for identifying therapeutic targets and charting research avenues to enhance our understanding of the intricate molecular mechanisms underlying hepatocellular carcinoma.

INTRODUCTION

Liver cancer is a significant global health concern, ranking as the fourth leading cause of cancer-related deaths. Hepatocellular carcinoma (HCC) accounts for approximately 85%−90% of primary liver malignancies, primarily caused by chronic infections from hepatitis B virus (HBV) and hepatitis C virus (HCV).[1] Other factors such as alcohol misuse and metabolic

Received: February 15, 2024
Revised: May 22, 2024
Accepted: May 24, 2024
Published: June 9, 2024

syndrome also contribute to its prevalence. While direct-acting antiviral therapy has effectively cured chronic HCV infection,[2] current antiviral measures only manage to control rather than fully eliminate HBV, affecting approximately 292000000 individuals worldwide.[3] Mass spectrometry (MS)-based proteomics plays a crucial role in assessing global protein abundance and post-translational modifications, providing insights that genomic analysis alone may not uncover. The combination of sequencing and MS offers a more comprehensive understanding, bridging the gap between cancer genotype and phenotype through functional proteomics and the elucidation of signaling networks. In a normal cell, approximately one-third of proteins are regulated by phosphorylation, which is one of the most important post-translational modifications. This modification plays a vital role in controlling numerous biological functions, including proliferation, cell division, apoptosis, and cell survival.[4] Proteins can shift between a dephosphorylated and phosphorylated state under the specific control of protein phosphatases and kinases. Dephosphorylation is catalyzed by protein phosphatases, while the phosphorylation of hydroxyl amino acid side chains is catalyzed by protein kinases.[5]

More recently, advancements in mass spectrometry-based methods have enabled comprehensive global proteome and phosphoproteome profiling, opening up new possibilities for research. In the context of HCC, two significant proteogenomic studies, both focusing on hepatitis B virus (HBV)-associated HCCs, have been published.[6] In the first study, authors conducted proteome and phosphoproteome profiling of early stage HBV-associated HCCs. Their findings revealed that a subset of HCCs exhibited disrupted cholesterol homeostasis and the overexpression of SOAT1, which was linked to poor patient outcomes. Notably, avasimibe, an inhibitor of SOAT1, demonstrated effectiveness in reducing tumor size in cases where SOAT1 was overexpressed. This was validated through patient-derived xenograft mouse models. In the second study, an integrated proteogenomic analysis of HBV-related HCC shed light on the activation status of key signaling pathways and metabolic reprogramming in these HCCs. Within this context, authors identified PYCR2 and ADH1A as essential proteins involved in the metabolic reprogramming of HCC. These proteins, found through proteomic analysis, also emerged as valuable prognostic biomarkers for HCC. These studies illustrate the power of proteogenomics and mass spectrometry-based approaches in enhancing our understanding of HCC, potentially leading to the development of targeted therapies and improved patient outcomes.

Alcohol dehydrogenases (ADHs) constitute a superfamily of dehydrogenase enzymes primarily located on chromosome 4q22−q24. This superfamily encompasses various classes, including class I (ADH1A, ADH1B, and ADH1C), class II (ADH4), class III (ADH5), class IV (ADH6), and class V (ADH7).[7] These ADH family members are broadly expressed across various human tissues, with the notable exception of ADH7, which is not expressed in the human liver.[7] Prior research has established a link between members of the ADH gene family and several types of cancers.[8] Furthermore, genetic variations within ADHs have been shown to influence cancer risk, particularly among individuals with alcohol dependence.[9,10] Recent investigations have shed light on the prognostic value of ADH family members in nonsmall cell lung cancer and gastric cancer.[11] However, the prognostic significance of ADH family members in HCC remains uncertain.

The immunosuppressive tumor microenvironment in HCC plays a critical role in tumor development. C-type (Ca^{2+}-dependent) lectin (CLEC) receptors, which are crucial for innate pattern recognition, have the potential to regulate immune cell trafficking and modulate the activity of cancer cells.[12] The CLEC family consists of numerous molecules, including CLEC1, CLEC2, CLEC4, and more. Substantial evidence indicates that CLECs play pivotal roles in activating and modulating the immune system.[13] However, there is currently limited information available regarding the expression and prognostic significance of CLECs in HCC. This suggests that the role of CLEC4G in HCC and its potential implications for patient outcomes have not been extensively studied and may require further investigation.

SATB2 (special AT-rich binding protein-2) is a transcription factor and epigenetic regulator known for its pivotal role in gene expression modulation. It wields influence over the expression of factors that maintain pluripotency and markers indicative of stem cells.[14] In mice, the absence of the SATB2 gene results in developmental defects in bone and osteoblast differentiation. SATB2 functions extend to craniofacial patterning, osteoblast differentiation, and the development of cortical neurons.[15,16] Moreover, SATB2 exhibits high expression levels in embryonic stem cells and progenitor cells, whereas its presence in normal human tissues is either minimal or absent. Recent research findings have underscored the transformative capacity of the SATB2 gene, which can convert normal epithelial cells into cancer stem-like cells in the context of pancreatic, colorectal, and breast cancer models.[17] Additionally, the expression of SATB2 is significantly elevated in cancer tissues when compared to their normal counterparts. Intriguingly, chronic exposure to ethanol and the presence of reactive oxygen species have been identified as inducers of SATB2 in pancreatic ductal epithelial cells, indicating that it can be regulated by stress and inflammation.[18] The comprehensive examination of differential expression and regulatory mechanisms linked to SATB2 in HCC remains an area yet to be fully explored.

Calcium/calmodulin-dependent kinase type II is overexpressed in the brain[19] and is crucial for synaptic plasticity, affecting learning in the hippocampus, cerebellum, and cortex. As a key mediator in calcium ion signaling, CAMK2 plays a vital role in connecting neurons to the external environment, primarily due to its abundant expression.[20] Each of the four different isoforms of CAMK2 (alpha, beta, gamma, and delta) is encoded by separate genes. The molecular mechanisms of CAMK2β regulation are still not fully understood. Several studies have demonstrated that CAMK2β plays structural and enzymatic roles in both hippocampal and cerebellar plasticity.[21] CAMK2β structural role arises from an additional domain in its variable region, known as the F-actin binding domain, allowing it to cluster with CAMK2A on the actin cytoskeleton. In addition to its actin-binding capacity, CAMK2β can bundle actin independently of its kinase activity.[22] The interaction of CAMK2β with F-actin is critical for hippocampal long-term potentiation by controlling the distribution of CAMK2A.[23] In the cerebellar parallel fiber−Purkinje cell synapse, CAMK2β plays both structural and enzymatic roles. Its absence leads to the reversal of plasticity polarity and significant deficits in cerebellar learning.[24] Additionally, previous study found elevated expression of CAMK2β in the amygdala of a rat depression model subjected to chronic mild stress.[25] To gain a comprehensive understanding of the regulatory mechanisms of CAMK2β as a potential drug target, it is essential to thoroughly

https://doi.org/10.1021/acsomega.4c01496
ACS Omega 2024, 9, 26075−26096

investigate protein expression alterations resulting from CAMK2β dysregulation. However, the specific effects of CAMK2β on HCC have not been fully elucidated.

The granin family proteins are named after their organellar origin and were proposed to participate in all three steps of regulated secretion.[26] Secretogranin III (SgIII), also known as chromogranin D (CHGD or CgD), has been reported to bind cholesterol and cargo molecules for granule biogenesis.[27] Secretogranin II (SgII), also known as chromogranin C (CgC or CHGC), was found to undergo liquid−liquid phase separation in vitro, likely contributing to the regulation of granule sizes.[27] Chromogranins A and B (CHGA and CHGB), formerly called CgA and CgB (SgI), respectively, were proposed to participate in protein aggregation-induced membrane budding in the trans-Golgi network (TGN).[28] Their roles in biogenesis are considered nonessential due to strong compensatory effects in CHGA/CHGB double knockout mice.[29] In typical secretory cells, CHGA and CHGB often stand out as the most prevalent members within the granin family of proteins. Despite their low sequence similarity, they are known to engage in interactions not only with each other but also with various partners.[30] While prior studies primarily emphasized the heat-stable soluble fractions of CHGB,[31] recent research has shed light on other facets of this protein. Partially purified native CHGB was discovered to bind to phospholipid vesicles in vitro.[32] Furthermore, a tightly membrane-associated form of CHGB was observed on the surface of PC-12 cells following stimulated granule release. This form was attributed to a fraction of the full-length protein that resisted membrane dissociation under challenging conditions, except for detergents.[33] Collectively, these findings suggest the potential existence of a membrane-inserted state of CHGB, at least partially, alongside its soluble forms. This duality implies that native CHGB might serve functions in both granular and plasma membranes. Several candidate markers have been associated with disease aggressiveness, including CHGB, which exhibits variations among different types of tumors. However, there is limited to no research related to CHGB in HCC. Further investigation is needed to elucidate its role in HCC. In general, greater expression of CHGA is observed in well-differentiated NETs compared to poorly differentiated NETs.[34]

Reprogramming of metabolism is one of the hallmarks of cancer. Cancer cells mainly rely on aerobic glycolysis to sustain cell proliferation. The increase in glucose uptake, even in the presence of oxygen, known as the Warburg effect, is more favorable for cancer cell proliferation.[35] Furthermore, glycogen is one of the crucial sources of glucose for cancer cells. It is a high molecular weight branched polysaccharide of glucose, serving as the primary glucose storage macromolecule in animals. Glycogen stored in the liver is essential for maintaining blood glucose levels.[36] Glycogen phosphorylase (GP) is the key enzyme responsible for the decomposition of glycogen in glycogen catabolism. GP has three isoforms such as PYGB, PYGL, and PYGM.[37] It is activated by phosphorylase kinase and allosteric stimulator glucose-6-phosphate (G6P) at Ser14. Previous studies have revealed significant insights into these isoforms. The absence of PYGL leads to an increase in reactive oxygen species clusters, cell death, and cell aging.[38] PYGB plays a crucial role in resistance, and inhibiting or losing PYGB leads to cell death in glucose starvation-resistant pancreatic cancer cells.[39] Additionally, another study demonstrated that the knockdown of the PYGB gene significantly inhibits the proliferation, migration, and invasion of ovarian cancer cells.[40] PYGM is typically associated with type V glycogen storage disease, a disorder of carbohydrate metabolism in skeletal muscle.[41]

A kinase anchor protein 12 (AKAP12), also recognized as Src-suppressed C-kinase substrate (SSeCKS), gravin, and AKAP250, belongs to the AKAP family and a vital component of the cytoskeletal structure. AKAP12 plays a crucial role in upholding cellular and tissue stability, as well as regulating cell proliferation and metastasis through the activating the phosphoinositide 3-kinase (PI3K)/protein kinase B (AKT) or protein kinase A (PKA)/protein kinase C (PKC) pathways. Remarkably, in HCC, AKAP12 is frequently downregulated due to promoter hypermethylation.[42,43] Additionally, its levels are diminished in hepatic cirrhosis and precancerous lesions, primarily attributed to the upregulation of microRNA (miR)-183 and miR-186, both of which target AKAP12. AKAP12 serves as a critical scaffold protein for maintaining cell structure and facilitating signal transduction. Nevertheless, the precise role of AKAP12 in HCC remains enigmatic. This study aims to unravel the potential impact of AKAP12 in HCC and illuminate its underlying molecular mechanisms.

CBFA2T3 (also known as ETO2 or MTG16) is a hematopoietic corepressor that forms stoichiometric complexes with E-proteins (e.g., E2A and HEB). These complexes facilitate the exchange of coactivators, including p300 and GCN5 histone acetyltransferases (HATs), as well as nuclear receptor corepressors (NCoR/SMRT) and HDACs.[44] Notably, CBFA2T3 plays a crucial role in hematopoietic transcriptional regulation and is frequently implicated in leukemogenic translocations that give rise to CBFA2T3 fusion proteins, such as RUNX1-CBFA2T3 in therapy-related AML.[45] Nevertheless, the role of CBFA2T3 in HCC has not been extensively studied and warrants further investigation. In this study, we demonstrate that CBFA2T3 is downregulated in tumor patients compared to nontumor patients.

SLC22A1, also known as Organic Cation Transporter 1 (OCT1), represents a highly expressed transporter in the human liver. Positioned on the sinusoidal membrane of hepatocytes, OCT1 plays a crucial role in facilitating the hepatic uptake of various small, positively charged hydrophilic compounds. This transporter exhibits poly specificity and is responsible for the transport of a diverse range of endogenous bioactive amines, such as dopamine, histamine, and serotonin.[46] SLC22A1 exhibits predominant expression in normal human liver, while SLC22A2 is predominantly expressed in the kidney. Notably, SLC22A1 mRNA expression is downregulated in HCC. However, the mechanisms underlying the altered expression of SLC22A1 in HCC compared to normal liver remain poorly understood. In previous studies, we have reported that alternative splicing of SLC22A1 pre-mRNA plays an essential role in the poor response of HCC to sorafenib, the first-line drug in the treatment of advanced HCC.[47] The downregulation of SLC22A1 correlates with worse patient outcomes and tumor progression. It is believed that the development of HCC is accompanied by aberrant SLC22A1 variants, which may significantly affect sorafenib levels within the affected intracellular concentrations in HCC.[48] However, there is still a lack of knowledge about how SLC22A1 affect the development and prognosis of HCC. The identification of prognosis-associated biomarkers is crucial to improve HCC patient survival. The present study aimed to explore potential predictive SLC22A1 biomarkers for HCC.

https://doi.org/10.1021/acsomega.4c01496
ACS Omega 2024, 9, 26075−26096

Table 1. Identified Significant Phosphoproteins and Corresponding Phosphosites in Linked to HCC (log_2 FC ≤ −2.0; p-Value < 0.0001) Using LIMMA Package in RStudio Software

no.	gene	log FC	sites	p-value	adj. p-value	change	Entrez ID
1	ADH1A	−2.9336	S365	1.90×10^{-36}	1.85×10^{-35}	down	124
2	ADH1B	−2.8314	S109	1.90×10^{-34}	1.85×10^{-33}	down	125
3	ADH1C	−2.1144	S165	5.55×10^{-61}	3.56×10^{-58}	down	126
4	ADH4	−2.6993	S278	4.24×10^{-56}	6.71×10^{-54}	down	127
5	ADH4	−2.1409	S330	4.94×10^{-53}	4.43×10^{-51}	down	127
6	AKAP12	−2.2447	S286	7.81×10^{-37}	8.00×10^{-36}	down	9590
7	CAMK2B	−2.5304	S411	3.77×10^{-52}	2.92×10^{-50}	down	816
8	CAMK2B	−2.7334	S454	3.37×10^{-21}	1.06×10^{-20}	down	816
9	CAMK2B	−2.7334	T341	3.37×10^{-21}	1.06×10^{-20}	down	816
10	CBFA2T3	−2.1983	S510	4.10×10^{-24}	1.56×10^{-23}	down	863
11	CBFA2T3	−2.2591	S564	6.53×10^{-43}	1.24×10^{-41}	down	863
12	CHGB	−2.3658	S130	2.37×10^{-49}	1.09×10^{-47}	down	1114
13	CHGB	−2.451	S225	5.28×10^{-38}	5.99×10^{-37}	down	1114
14	CHGB	−2.5344	S391	4.16×10^{-44}	9.42×10^{-43}	down	1114
15	CLEC4G	−4.5284	S12	7.71×10^{-26}	3.29×10^{-25}	down	339390
16	PYGL	−2.4327	S605	6.82×10^{-70}	7.87×10^{-66}	down	5836
17	SLC22A1	−2.1096	S321	5.73×10^{-33}	4.15×10^{-32}	down	6580
18	SLC22A1	−2.2795	T541	4.77×10^{-25}	1.94×10^{-24}	down	6580
19	STAB2	−3.526	S2497	9.86×10^{-37}	1.00×10^{-35}	down	55576

Certainly, despite the wealth of available information, the mechanisms governing the differential expression and regulation of these genes in HCC have remained unexplored. Additionally, the roles of STAB2, CHGB, CBFA2T3, AKAP12, and CLEC4G in HCC have not been previously investigated. Therefore, the primary objective of this study was to assess whether STAB2, ADHs, CHGB, CBFA2T3, AKAP12, PYGL, CHGB, CAMK2β, and CLEC4G gene expression could serve as novel biomarkers for HCC. Furthermore, it is important to note that a detailed examination of the immunohistochemical expression of SATB2 and CLEC4G in HCC had not been conducted previously. As of the present, the U.S. Food and Drug Administration (FDA) has granted approval for more than two dozen small-molecule protein kinase inhibitors and six therapeutic antibodies targeting protein kinases for clinical application. These approvals have primarily focused on targeted cancer treatments. Furthermore, alongside these FDA-endorsed medications, numerous other protein kinase inhibitors are currently undergoing evaluation in clinical trials. It is worth noting that a variety of small-molecule agents with the capacity to modulate kinases activity, either by activation or inhibition, have been developed. These agents show therapeutic potential for addressing various human ailments.

Disruptions in protein phosphorylation and dephosphorylation processes, including imbalances, can contribute to the development of various diseases, such as cancer, neurodegenerative disorders, and metabolic diseases.[4] In this study, our aim was to explore the roles of these genes in HCC through the integration of clinical data and advanced bioinformatics analyses. We conducted a retrospective analysis involving 159 patients diagnosed with HCC to gain insights into the dynamics of this condition. We compared gene expression levels in HCC tissues and non-HCC tissues and utilized bioinformatics tools and publicly available databases to analyze clinical data and patient survival outcomes, stratifying them based on low and high expression levels of these genes. We further validated our findings by examining differential gene expression profiles between HCC and non-HCC tissues, strengthening the association of these genetic variations with patient survival rates. To uncover the underlying mechanisms, we employed a variety of bioinformatics programs, revealing potential pathways and specific targets that could illuminate the roles of STAB2, ADHs, CHGB, CBFA2T3, AKAP12, PYGL, CHGB, CAMK2β, and CLEC4G in the context of HCC. It is worth noting that the protein expression and phosphorylation sites of these genes has not been comprehensively investigated in the context of HCC, making our study a valuable contribution to this area of research.

MATERIALS AND METHODOLOGY

Data Set Collection and Preprocessing. We collected proteomic and phosphoproteomic data sets from the publicly available Clinical Proteomic Tumor Analysis Consortium (CPTAC) database (https://pdc.cancer.gov), which provides mass spectrometry-based discovery proteomics. Our study involved a comparative analysis of clinical data and patient survival outcomes based on low and high expression levels of proteins. This analysis utilized bioinformatics tools and public databases. Furthermore, we investigated the differential expression between HCC tissues and non-HCC tissues. Subsequently, we validated the survival rates of patients with low or high protein expression. To gain insights into potential pathways associated with these findings, we employed a variety of bioinformatics programs. It is worth noting that the three databases (CPTAC, The Cancer Proteome Atlas (TCPA), and The Cancer Genome Atlas (TCGA)) are publicly accessible and open source. This study strictly adhered to the data access policies and publishing guidelines of these databases, obviating the need for local ethics committee approval.

Bioinformatics and Expression Analysis. The acquired data sets present details on phosphorylation site levels and total protein abundances across samples, derived from TMT 11 labeling experiments. Following normalization, we calculated relative abundances as log ratios (base 2) in comparison to the pooled reference samples. The genes were filtered based on criteria of log_2 FC ≤ −2 and adjusted p-values < 0.001, indicating downregulation. Our data analysis was performed using RStudio software.

https://doi.org/10.1021/acsomega.4c01496
ACS Omega 2024, 9, 26075−26096

Identification of Differentially Expressed Phosphorylation Sites. We performed a paired *t* test analysis utilizing the LIMMA package within the R/Bioconductor environment to discern differentially expressed phosphorylation sites between tumor and corresponding nontumor liver tissues. To address multiple hypothesis testing concerns, we applied the Benjamin−Hochberg false discovery rate (FDR) correction to adjust the *p*-values. Our criteria for significance involved adjusted *p*-values < 0.001 and $\log_2$ FC ≤ -2, serving as benchmarks to identify statistically significant differences. Applying adjusted *p*-values < 0.001 during differential gene screening allowed us to effectively control the false positive rate. Our primary focus in this study was on 12 distinct proteins and their associated phosphosites, demonstrating notable differences between tumor and nontumor liver tissues, all of which are documented in detail in Table 1 and Table S1. The generation of heat and volcano maps was facilitated using the gplots package within RStudio software.

Functional Enrichment Analysis and Pathway of Differentially Expressed Phosphorylation Sites. Our methodology adheres to a systematic pipeline tailored for data interpretation and visualization, empowering us to derive valuable insights into the functional implications of the identified differentially expressed phosphorylation sites. Gene ontology (GO) serves as a framework for delineating the functions of gene products across organisms and for identifying characteristic biological properties within high-throughput transcriptome data from genomes. We combined pathway enrichment analysis with visualization techniques, including heatmaps, to unravel the contributions of these sites to specific biological processes, cellular components (CC), and molecular functions (MF), such as the regulation observed in pathway enrichment analysis. Leveraging the Cluster Profiler R package, we conducted pathway enrichment analysis to annotate and functionally interpret the differentially expressed phosphorylation sites by associating them with established pathways and biological functions using gene set enrichment analyses (GSEA).

Overall Survival Analysis of the Hub Genes in HCC. The survival data extracted from the HCC patients within the CPTAC data set underwent Kaplan−Meier survival analysis and the log-rank test to assess the potential correlation between candidates and HCC outcomes. These analyses utilized the survival and survminer packages. Groups with low and high expressions were classified based on a median cutoff of 50% expression. We visualized the expression levels of the identified phosphorylation sites and their associated proteins using the *ggplot2* package. Moreover, we extended the analysis using the proteomics data to further investigate and analyze the phosphoproteomics results. Survival analysis was conducted on the proteins, and those showing a correlation with patient survival were retained for subsequent analyses. All statistical computations and analyses were performed using RStudio software.

Utilizing a 12-Gene Signature as an Independent Predictor for Overall Survival. We performed both univariate and multivariate Cox regression analyses to ascertain the prognostic model independence from other clinicopathological variables. These variables included age, gender, tissue registration, pathological stage, T staging, and the risk score for HCC patients. In these analyses, clinical features served as independent variables, while overall survival (OS) was considered the dependent variable for calculating hazard ratios (HR), along with its respective 95% confidence interval and a two-sided *p*-value.

Validation of the 12-Gene Signature Using Multiple Databases. We conducted an mRNA expression analysis of the gene signature in both HCC tissues and normal liver tissues using the Oncomine online microarray database (http://www.oncomine.org).[42] The analysis employed specific threshold settings: *p*-value < 0.01, a fold change > 2, and a gene rank within the top 10%. Data sets were meticulously selected based on statistical differences, encompassing sample size, fold change, *t* test results, analysis type, and *p*-values. Moreover, to assess protein expression levels associated with the gene signature, we retrieved immunohistochemical images from publicly available human protein maps via the Human Protein Atlas (http://www.proteinatlas.org).[43] This step further enriched the validation process. Additionally, to corroborate our findings, we acquired an independent HCC cohort from the International Cancer Genome Consortium (ICGC). Subsequently, we extracted the expression levels of the 12-gene signature and conducted a comparative analysis between HCC and nontumor tissues. The statistical analysis involved employing the Wilcoxon signed-rank test, and significance was determined at two-sided *p*-values less than 0.05, indicating substantial differences. Our utilization of the Human Protein Atlas (HPA) allowed us to discern the variations in key gene expression between HCC and nontumor tissues, further validating our investigation.

Creation and Assessment of Nomograms for Predicting HCC Survival. Nomograms serve as efficient tools in predicting cancer patient prognosis by simplifying complex statistical models into user-friendly charts. These aid in evaluating an individual's probability of OS.[44] Our study integrated all independent clinical and pathological prognostic factors identified via Cox regression analysis to construct a nomogram. This nomogram estimates OS probabilities at 1, 3, and 5 years for HCC patients. We assessed the nomogram's accuracy by comparing predicted probabilities with observed actual probabilities through a calibration curve. An overlapping curve with the reference line indicates model accuracy. Additionally, ROC analysis was performed to compare prediction accuracy between the combined model's nomogram and individual nomograms for each clinical and pathological prognostic factor.

Hub Genes and Drug Interaction Analysis. Drugs targeting hub genes associated with HCC were identified utilizing the Drug Gene Interaction Database (DGIdb v3.0.2). DGIdb serves as a user-friendly platform for mining drug-gene interactions and the druggable genome data, amalgamating information from over 30 credible sources such as Ensembl, ChEMBL, DrugBank, PubChem, NCBI Entrez, clinical trial databases, PharmGKB, and NCBI PubMed literature references.[49] To ensure reliability, drugs supported by multiple databases or substantiated by PubMed references were selected. Furthermore, only drugs approved by the FDA were considered for further investigation. Additionally, the Search Tool for Interacting Chemicals (STITCH v5.0;) was employed to visualize the interaction network of the hub genes and identify potential drug interactions. STITCH integrates diverse data sources encompassing more than 430000 chemicals.[49]

RESULTS

CPTAC Patient Characteristics. We acquired data from the CPTAC database, comprising phosphoproteomics and proteomics data sets and clinical information from 159 patients treated at the Department of Hepatobiliary Surgery, forming the basis for our proteogenomic analysis. The collected clinical data

https://doi.org/10.1021/acsomega.4c01496
ACS Omega 2024, 9, 26075−26096

Table 2. HCC Patient Information Summary in the CPTAC Database

parameter	mean	coef	exp(coef)	exp(−coef)	se(coef)	z	p-value	lower 0.95	upper 0.95
gender	NA	0.329	1.390	0.7200	0.335	0.983	0.3258	0.7211	2.6752
age	53.872	0.001	1.000	0.9992	0.011	0.068	0.8396	0.9800	1.0219
PTT	12.009	−0.003	0.997	1.0027	0.065	−0.042	0.9666	0.8790	1.1316
TB	12.016	−0.047	0.954	1.0484	0.030	−1.566	0.1174	0.8993	1.0117
ALB	40.486	0.032	1.030	0.9689	0.038	0.836	0.4032	0.9591	1.1106
ALT	50.216	0.000	1.000	1.0003	0.003	−0.105	0.9166	0.9945	1.0050
GGT	79.709	−0.001	0.999	1.0007	0.002	−0.365	0.7154	0.9958	1.0029
AFP	6795.462	0.000	1.000	1.0000	0.000	0.403	0.6869	1.0000	1.0000
medical history of liver cirrhosis	NA	−0.563	0.569	1.7563	0.280	−2.015	0.0439	0.3293	0.9844
tumor size cm	6.568	0.056	1.060	0.9452	0.040	1.398	0.1622	0.9777	1.1447
number of tumors	1.642	−0.044	0.957	1.0448	0.111	−0.396	0.6923	0.7694	1.1905
tumor.differentiation	2.385	−0.166	0.847	1.1803	0.258	−0.644	0.5193	0.5114	1.4038

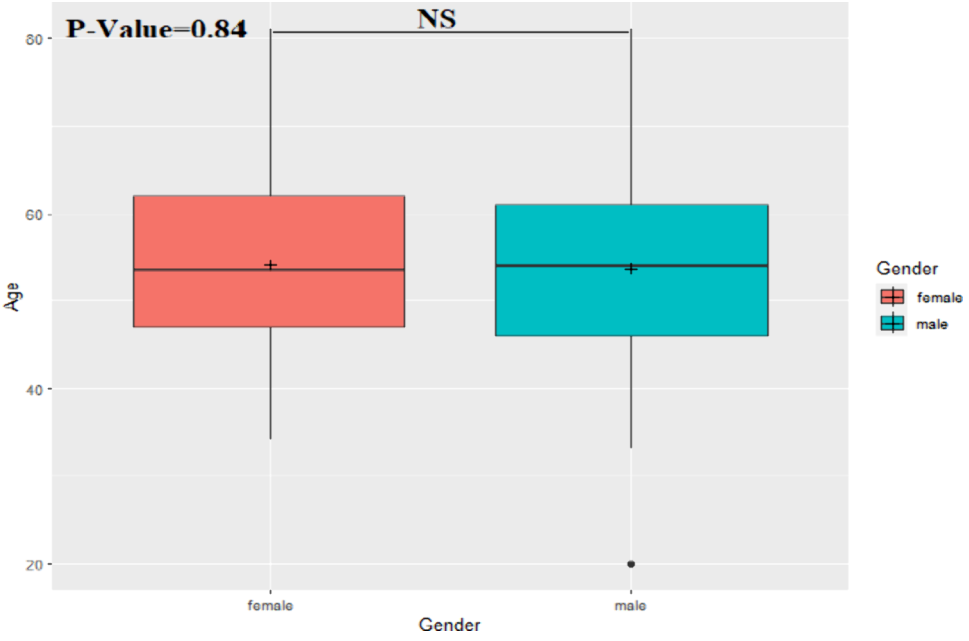

Figure 1. Correlation between age and gender among HCC patients, revealing a corresponding p-value of 0.84 (NS = not significant).

included gender, age, family history of liver cancer, presence of liver cirrhosis, alpha-fetoprotein (AFP) levels, tumor size, tumor number, and various biochemical parameters (such as total bilirubin (TBil), partial thromboplastin time (PTT), gamma-glutamyl transferase (GGT), alanine aminotransferase (ALT), and albumin (ALB)) as detailed in Table S2 (patient information). Throughout the study period, all participants were continuously monitored until death or loss to follow-up in accordance with the study protocol. This extensive data set enabled a comprehensive exploration of the proteogenomic landscape, specifically focusing on 12 proteins and their correlation with clinical information.

Clinical Application in HCC. Table 2 illustrates a comparative analysis of general clinical data between two participant groups. The comparison encompassed various parameters, such as gender, presence or absence of liver cirrhosis, age, AFP levels, TBil levels, tumor size, tumor number, PTT, GGT, ALT levels, and ALB. No statistically significant differences were observed for these parameters (all $p > 0.05$), indicating similar distributions among the participant groups. However, a notable finding emerged regarding the presence of a family history of liver cancer ($p < 0.05$), revealing a statistically significant difference between the groups. Additionally, Figure 1 depicts the correlation between age and gender in HCC patients, yielding a corresponding p-value of 0.84. This nonsignificant p-value suggests that gender alone does not significantly influence prognosis within this data set. Although a slight difference in survival probability for females was observed, it did not attain statistical significance.

Identification of Dysregulated Phosphosites by In-Depth Phosphoproteomics Analysis. We conducted a thorough analysis of phosphosite abundance across 159 pairs of tumor and adjacent nontumor samples, encompassing a total of 11549 phosphorylation sites related to 4043 phosphoproteins. Impressively, these sites were quantified in at least half of the samples, with 9994 demonstrating substantial differential expression. In this analysis, we observed 8198 sites significantly upregulated, while 1796 sites were downregulated in tumor samples compared to their nontumor counterparts. Our differentiation criteria relied on a paired two-sided Student's t test, and significance was determined with Benjamini–Hochberg (BH) adjusted p-values < 0.001.

Further scrutiny unveiled 19 phosphorylation sites (corresponding to 12 unique genes) exhibiting notable changes (p-values < 0.001) between samples. For enhanced visualization, we employed RStudio software, generating both volcano and

https://doi.org/10.1021/acsomega.4c01496
ACS Omega 2024, 9, 26075−26096

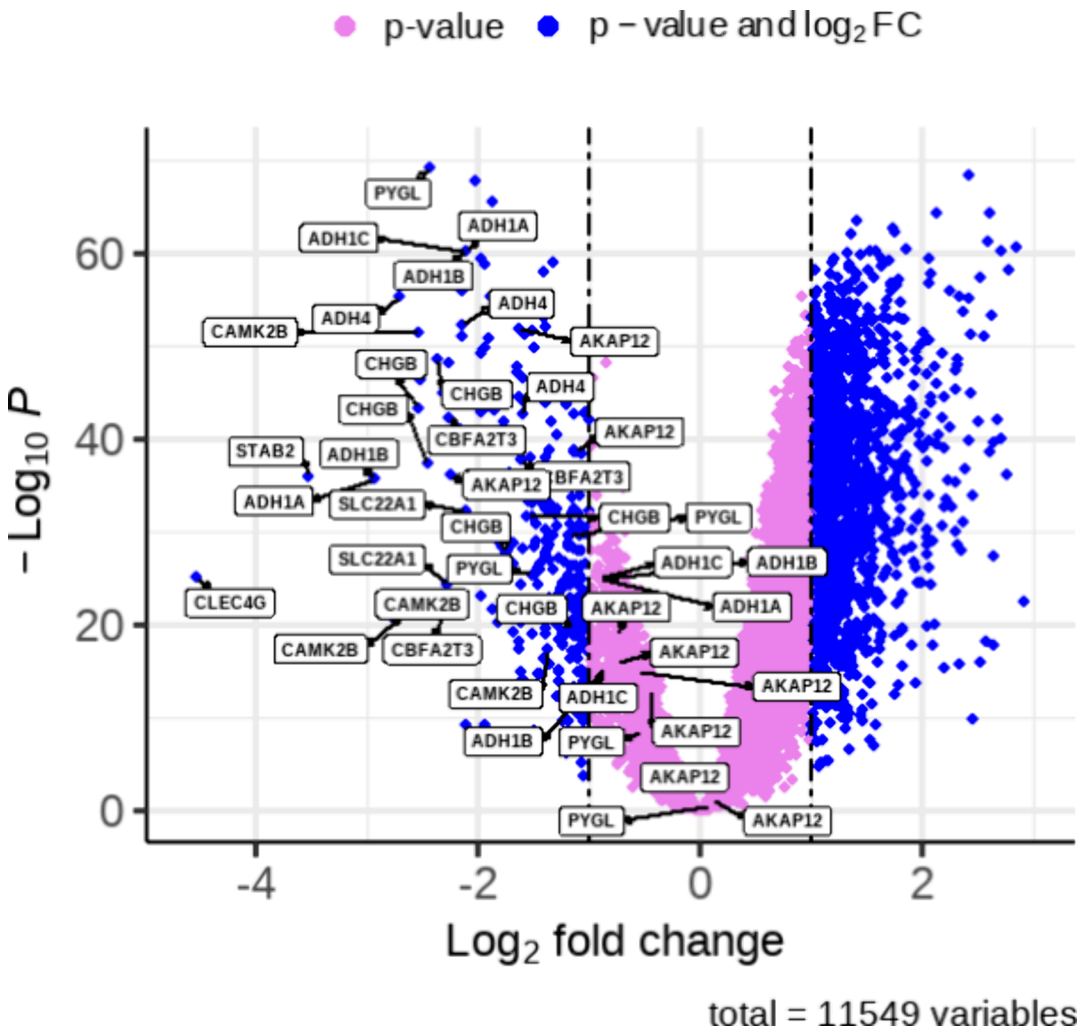

Figure 2. Volcano plot illustrating differential gene expression in hepatocellular carcinoma samples. On the left side, 12 genes along with their corresponding phosphosites (with $\log_2$ FC ≤ -2 and a p-value < 0.001) are labeled with gene names. Genes showing decreased expression are indicated in blue on the left, while up-regulated genes are depicted in blue on the right.

heatmap plots to elucidate our findings. Specifically, our results emphasized that 12 genes exhibited statistically significant downregulation, evident in the volcano plot showcased in Figure 2. To identify differentially expressed proteins in the CPTAC database, we utilized criteria involving $\log_2$ FC ≤ -2 and a p-value < 0.001, denoting statistical significance.

Functional Annotation, Pathway Exploration, and Visual Representation. We conducted an in-depth analysis of Kyoto Encyclopedia of Genes and Genomes (KEGG) pathways for the identified phosphoproteins, encompassing both upregulated (8198) and downregulated (1796) entities, using over-representation analysis (ORA) via Cluster Profiler in RStudio. Additionally, GSEA were performed for both GO and KEGG pathways, focusing on 12 downregulated genes and their differentially expressed genes (DEGs). The GO analysis unveiled pivotal biological processes (BP), emphasizing ethanol metabolic, retinol metabolic, retinoid metabolic, primary alcohol metabolic, and retinoic acid metabolic processes. Molecular function (MF) assessments indicated enrichments in alcohol acid dehydrogenase [NAD(P)+] activity, NAD-retinol dehydrogenase, oxidoreductase activity, monosaccharide binding, and vitamin binding among the 12 phosphoproteins, as depicted in Figure 3 and Table S3 (GO-GSEA). Regarding cellular component (CC) analysis, the identified locations for these proteins included cytosol, plasma membrane, nucleoplasm, and endocytic vesicle membrane. In our KEGG pathway analysis, we identified significant pathways such as tyrosine metabolism, fatty acid degradation, retinol metabolism, alcohol liver disease, drug metabolism cytochrome P450, and pyruvate metabolism. These findings were further supported by functional GSEA, emphasizing the importance of glucagon signaling and glycolysis/gluconeogenesis, as visually represented in Figure 4A. We closely examined disease−gene associations for the 12 downregulated genes and discovered prevalent connections with conditions such as pharyngeal carcinoma, malignant neoplasm of pharynx, alcohol-induced disorders, alcoholic liver disorders, pancreatitis, hazardous drinking, autosomal dominant hypocalcemia, and liver cirrhosis as shown in Figure 4B. Additionally, we utilized the pmcplot function to visualize publication trends extracted from PubMed Central, which aided in selecting pathways for further investigation. This visualization method helped determine the number and proportion of publications related to our query, illustrated in Figure 5. Collectively, these comprehensive analyses revealed pivotal pathways and trends, providing valuable insights into potential connections between phosphorylated proteins and HCC.

Protein−Protein Interaction Network and Identification of Genes Hub. We utilized the Search Tool for the

https://doi.org/10.1021/acsomega.4c01496
ACS Omega 2024, 9, 26075−26096

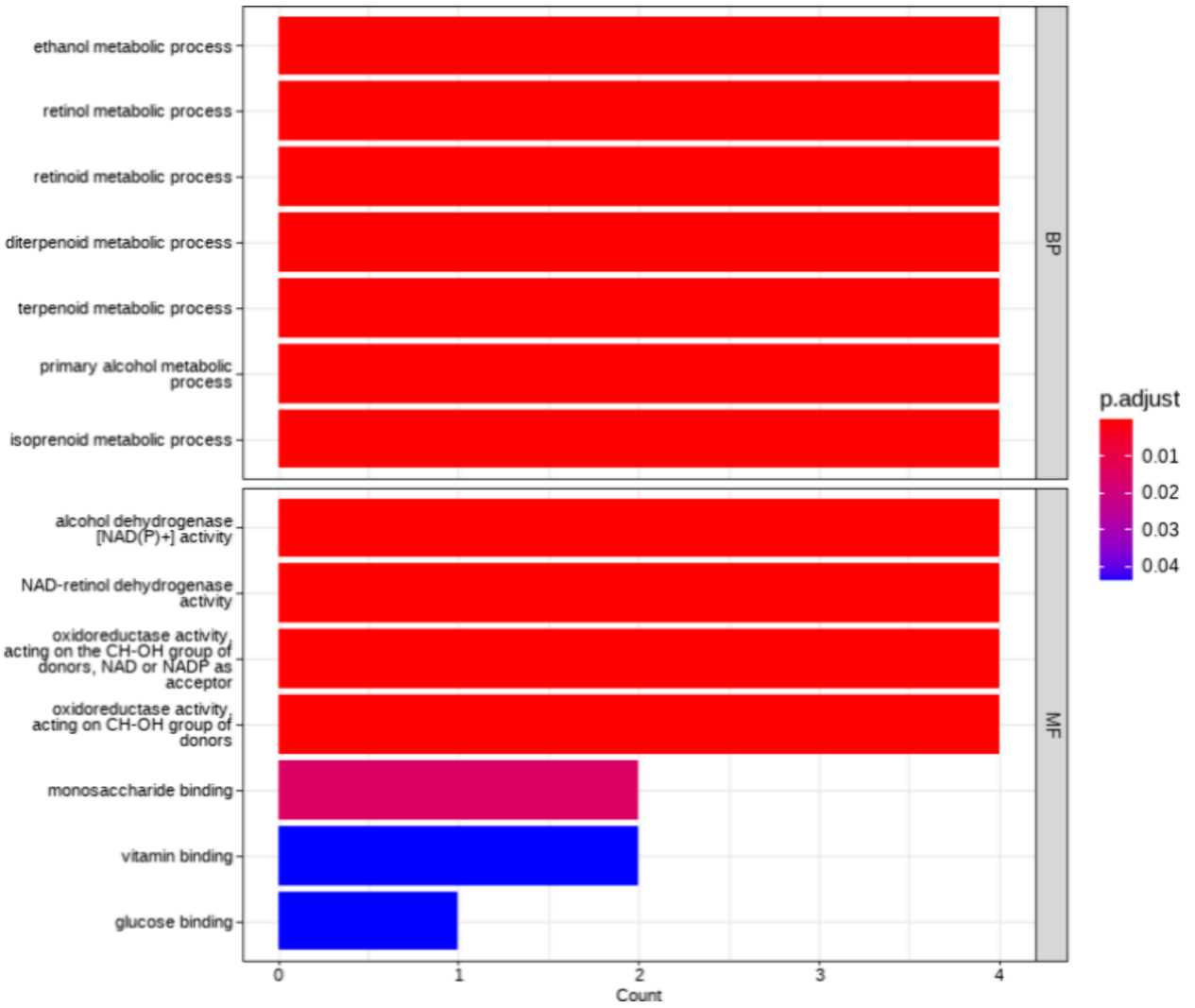

Figure 3. GO analysis for 12 significant genes correlated with genes in the high-risk group within the red module, revealing significant BP and significant MF.

Retrieval of Interacting Genes/Proteins (STRING) to construct a protein−protein interaction (PPI) network for exploring relationships among differentially expressed proteins at the protein level. Understanding protein interactions is vital for deciphering the metabolic and molecular mechanisms underlying tumors. The network encompassed 12 significant proteins along with their phosphosites, reaching a confidence score of 200 at the protein level. Illustrated in Figure 6, our constructed PPI network consisted of 12 nodes, 8 edges (representing interactions), and 2 expected interactions (p-value = 0.00032). Leveraging the STRING database, we visualized this PPI network using RStudio software. Our in-depth analysis identified ADH1A, ADH1B, ADH4, ADH1C, CLEC4G, STAB2, CAMK2B, and CHGB as highly connected hub genes, having the highest scores. These findings, along with their FDR, p-values, and enriched pathways obtained from the STRING network analysis using RStudio software, are meticulously presented in Table 3.

Time-Dependent ROC Curves and Kaplan−Meier Analysis Based on a Gene Signature. We employed the Kaplan−Meier survival curve to compare the OS between two groups, stratified based on their median risk scores as depicted in Figure 7. Additionally, we assessed the prognostic capability of the 12 gene signature using the area under the time-dependent ROC curve (AUC). A higher AUC value denotes superior model performance. Our analysis revealed a significant difference in OS between the high-risk and low-risk groups (p-value < 0.05). Notably, individuals exhibiting high expression levels of ADH1A, ADH4, ADH1C, and SLC22A1 demonstrated lower OS rates compared to those with lower expression levels ($p \leq 0.05$). However, we did not observe a significant correlation between the expression of other genes ($p > 0.05$), as demonstrated in Figure 8. Consequently, ADH1A, ADH4, ADH1C, and SLC22A1 were identified as key genes. Further examination unveiled that the expression levels of ADH1A (HR = 0.7; $p = 0.046$), ADH4 (HR = 0.49; $p = 1 \times 10^{-4}$), ADH1C (HR = 0.62; $p = 0.0082$), and SLC22A1 (HR = 0.52; $p = 3 \times 10^{-4}$) were strongly associated with higher survival rates among HCC patients. These findings suggest that lower expression levels of these four genes at diagnosis may serve as adverse prognostic markers, potentially leading to reduced OS in HCC patients. In the analysis of DFS, we categorized gene expressions of HCC patients into low-expression and high-expression groups (cutoff-high at 50%, cutoff-low at 50%). The results depicted in Figure 9 indicated significantly higher survival probabilities associated with lower expression levels ($P < 0.05$).

https://doi.org/10.1021/acsomega.4c01496
ACS Omega 2024, 9, 26075−26096

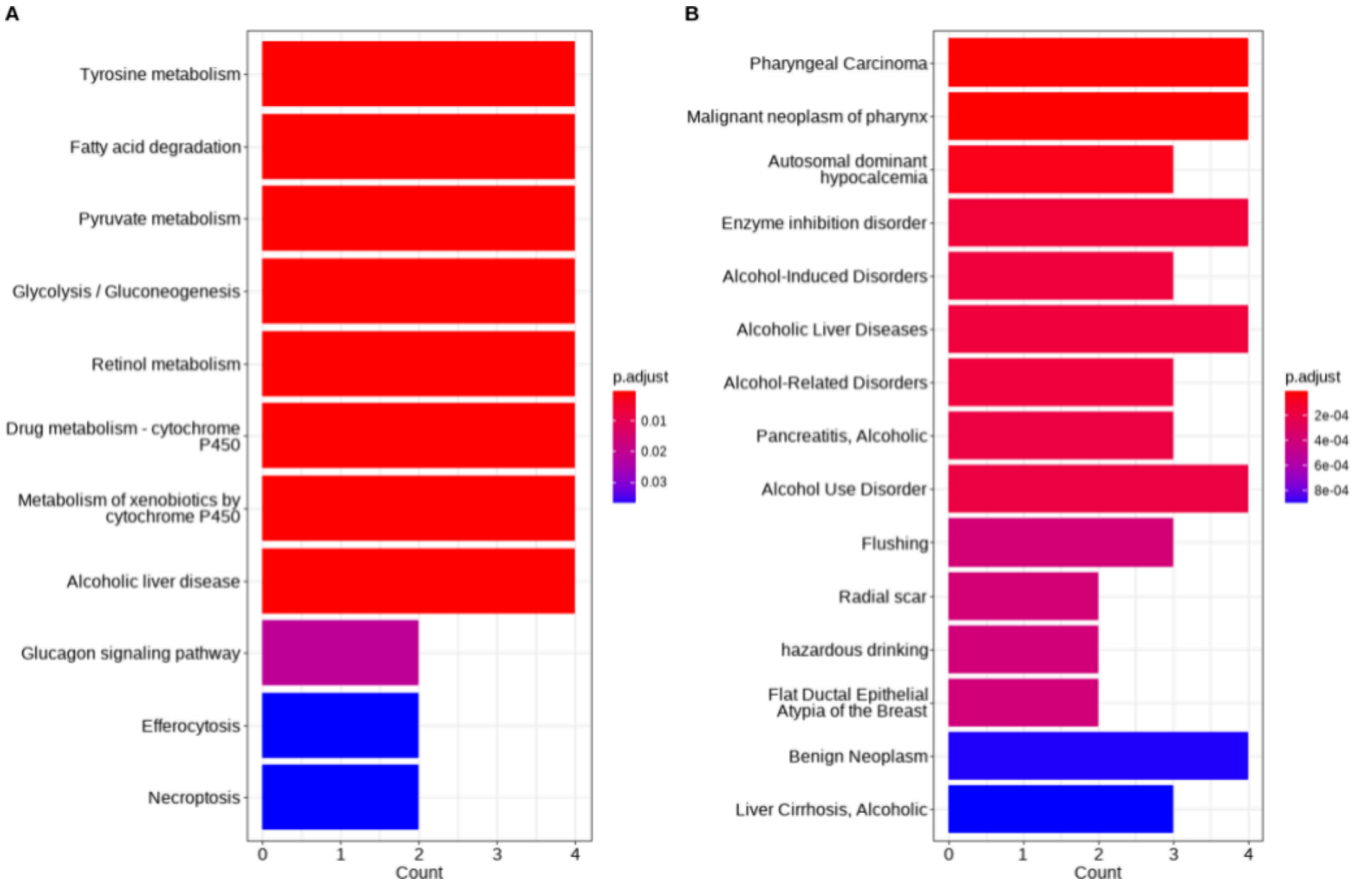

Figure 4. A) KEGG pathway enrichment of 12 significant phosphoproteins (downregulated). B) Disease−gene associations correlated with genes in the high-risk group within the red module.

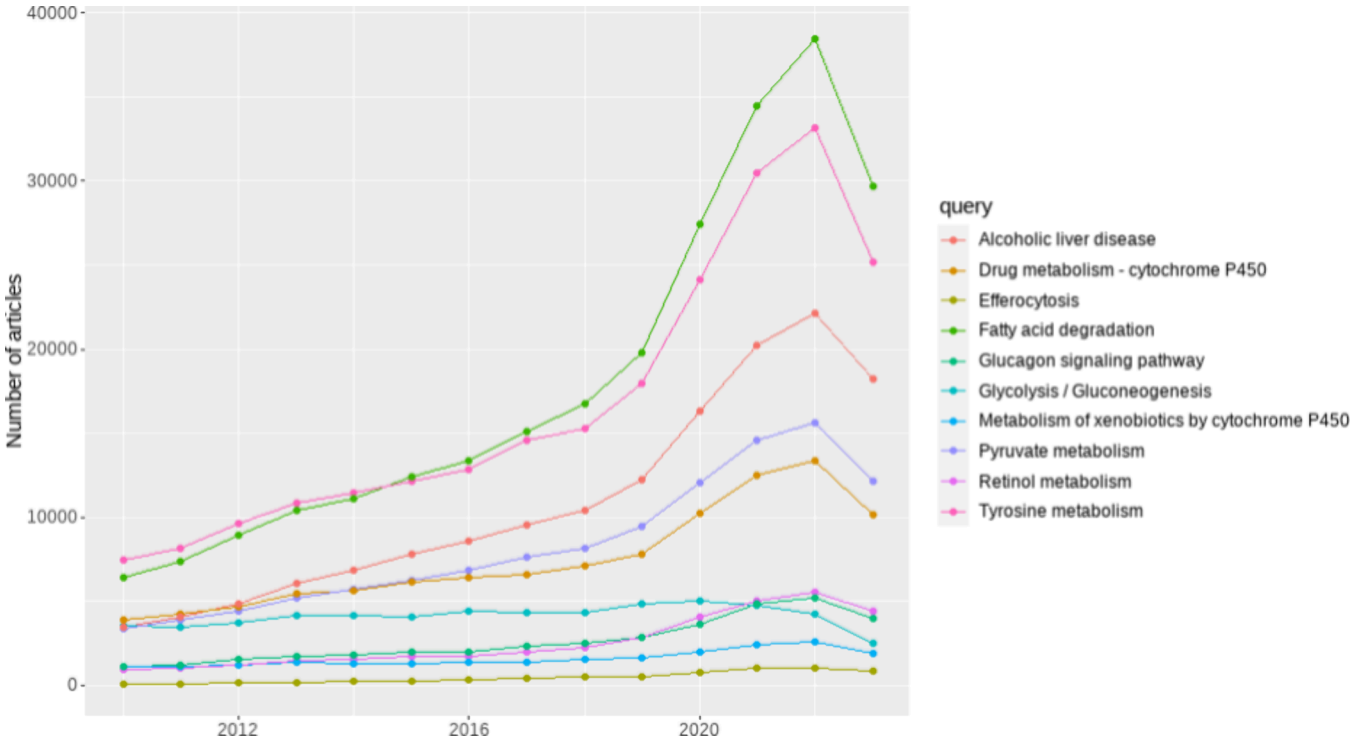

Figure 5. PmcPlot of enrichment analysis of 12 significant proteins.

Specifically, CAMK2β (HR = 0.64; p = 0.004), ADH4 (HR = 0.52; $p = 1.8 \times 10^{-5}$), and SLC22A1 (HR = 0.67; p = 0.009) were strongly correlated with enhanced survival rates among HCC patients. Furthermore, the survival curve analysis for both

https://doi.org/10.1021/acsomega.4c01496
ACS Omega 2024, 9, 26075−26096

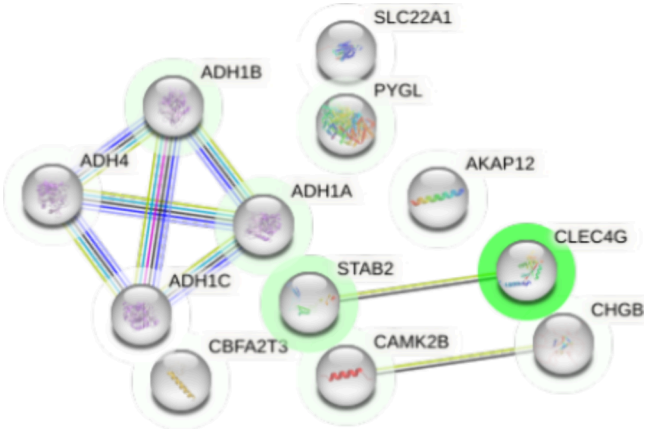

Figure 6. PPI network of 12 significant phosphoproteins (down-regulated proteins) with connection line thickness indicating betweenness, node color gradients representing log FC change, and green denoting coexpression nodes from the STRING database.

OS and DFS underscored the efficacy of these genes in predicting prognosis among HCC patients.

Hub Genes and Drug Interaction Analysis. We investigated 12 hub genes to explore potential drug interactions using the DGIdb database. This analysis revealed a set of 60 drugs that could potentially be effective in treating HCC by targeting these 12 hub genes. This information was depicted and screened through the DGIdb database. To refine our selection, we exclusively compiled FDA approved drugs, focusing specifically on three promising targets: SLC22A1, CAMK2β, and AHD1A. Among these targets,

we identified four FDA approved drugs Imatinib, Sorafenib, Cytarabine, and Fludarabine that exhibited shared functionality in regulating the features of SLC22A1, CAMK2β, and AHD1A. **Imatinib** mesylate is a protein and tyrosine kinase inhibitor derivative of 2-phenylamino-pyrimidine. Initially developed to target the platelet-derived growth factor receptor,[50] it has since been discovered to effectively inhibit other protein tyrosine kinases like c-kit (associated with gastrointestinal stromal tumors) and the BCR-ABL fusion protein (found in Philadelphia chromosome chronic myelogenous leukemia). These protein tyrosine kinases collectively phosphorylate specific amino acids on substrate proteins, initiating signal transduction pathways that alter cell biology. This includes impacting cell growth, differentiation, and apoptosis. When constitutively activated, whether through mutation or other mechanisms, these kinases can contribute to the development of malignancies.[51]

Sorafenib, an oral multikinase inhibitor, has been the established standard of care for patients with advanced unresectable HCC since 2007. Its mechanism involves the inhibition of several tyrosine kinases that play crucial roles in tumor angiogenesis and progression, targeting vascular endothelial growth factor receptor (VEGFR-2/3), platelet-derived growth factor receptor (PDGF-R), Flt3, c-Kit, and Raf kinases within the MAPK/ERK pathway.[52] Currently, Sorafenib stands as the global standard treatment for advanced HCC, supported by evidence from two extensive randomized trials. Both trials demonstrated a notable improvement in OS compared to the placebo.[53] Despite its extensive use, the exact molecular mechanisms underlying sorafenib's activity remain incompletely understood. Additionally, several FDA approved drugs, including Idarubicin, Fludarabine, and Cytarabine, might potentially target ADH1A. Our study highlights various drugs that could potentially target CAMK2B to inhibit its function. Among these drugs, Cediranib, Cenisertib, Linifanib, and SNS-314 are currently under clinical trial investigation as they have not yet received FDA approval. **Linifanib** (ABT-869) serves as a distinctive ATP-competitive inhibitor, targeting all VEGF and PDGF receptor tyrosine kinases, while displaying limited activity against typical cytosolic tyrosine kinases and serine/threonine kinases.[54] In clinical trials, linifanib has exhibited notable efficacy as a monotherapy in individuals with advanced HCC.[55] Linifanib and sorafenib had similar OS in advanced HCC. Notably, we did not find any drugs specifically targeting and inhibiting the functionality of STAB2, CLEC4G, CHGB, CBFA2T3, PYGL, and AKAP12 within the DGIdb database. Further studies and research efforts are required to delve deeper into these genes, potentially leading to the development of drugs targeting their specific functionalities. Additionally, recent FDA approvals include Nivolumab (2017), Pembrolizumab (2018), and the combination of Nivolumab plus Ipilimumab (2020). Overall, these data might provide novel insight for targeted therapy in HCC patient and these findings are visually represented in Table 4.

Immunohistochemistry Analysis. The Human Protein Atlas (HPA) (http://www.proteinatlas.org) is an extensive resource offering immunohistochemistry-based expression data for various tissues and cell lines. In our investigation, we leveraged immunohistochemistry images to directly compare the protein expression of 12 genes between normal liver tissues and those affected by HCC, as depicted in Figure 10. Intriguingly, we observed high to medium expression levels of CAMK2β, STAB2, and CBFA2T3 proteins in HCC tissues, despite their absence in normal liver tissues. Moreover, AHD1A, AHD1B, AHD1C, AHD4, SLC22A1, and PYGL were detected

Table 3. KEGG Pathways Identified through the STRING Network Analysis Pertaining to the 12 Significant Genes Utilizing RStudio

no.	category	term	number of genes	number of genes in background	NCBI taxon Id	*p*-value	FDR	description
1	KEGG	hsa00071	4	42	9606	1.30×10^{-08}	2.21×10^{-06}	fatty acid degradation
2	KEGG	hsa00350	4	35	9606	6.58×10^{-09}	2.21×10^{-06}	tyrosine metabolism
3	KEGG	hsa00010	4	65	9606	6.85×10^{-08}	7.22×10^{-06}	glycolysis/gluconeogenesis
4	KEGG	hsa00830	4	64	9606	6.45×10^{-08}	7.22×10^{-06}	retinol metabolism
5	KEGG	hsa00980	4	69	9606	8.61×10^{-08}	7.22×10^{-06}	metabolism of xenobiotics by cytochrome P450
6	KEGG	hsa00982	4	64	9606	6.45×10^{-08}	7.22×10^{-06}	Drug metabolism - cytochrome P450
7	KEGG	hsa05204	4	75	9606	1.19×10^{-07}	7.22×10^{-06}	chemical carcinogenesis
8	KEGG	hsa01100	5	1447	9606	0.0011	0.0476	metabolic pathways

https://doi.org/10.1021/acsomega.4c01496
ACS Omega 2024, 9, 26075−26096

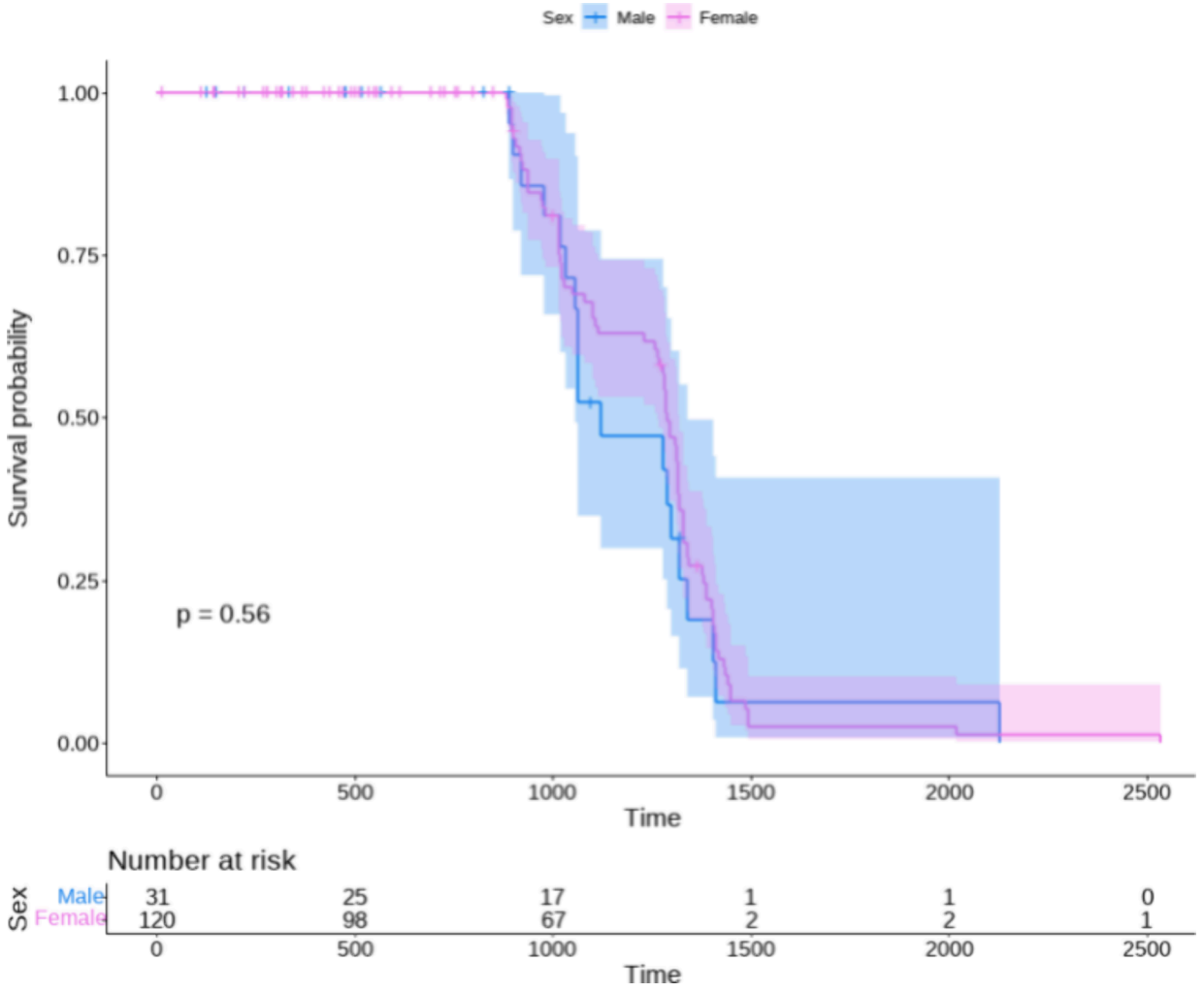

Figure 7. Kaplan−Meier OS plots and number at risk in HCC generated through the RStudio. Dashed lines represent the upper and lower confidence intervals.

in both normal and tumor tissues. In contrast, CLEC4G, CHGB, and AKAP12 were not identified in either normal liver tissues or HCC tissues.

DISCUSSION

HCC ranks as the sixth most common cancer globally. Over the past two decades, substantial advancements have been made in HCC treatment approaches, encompassing surgical resection, ablation, liver transplantation, and targeted therapies. Despite these strides, the 5-year survival rate for HCC remains suboptimal. Radiotherapy is generally avoided due to potential liver toxicity, and the utility of liver transplantation faces constraints, such as a shortage of available liver donors, limited success beyond Milan criteria, and challenges posed by etiological factors, especially the high relapse rate associated with HCV infection. HCC, marked by a high mortality rate, poses an ongoing challenge in the quest for effective biomarkers for treatment. Posttranslational protein modifications alter protein functions and interactions by modifying protein structures. Phosphorylation and dephosphorylation, reversible posttranslational modifications, predominantly regulate intracellular signaling pathways, impacting over 70% of cellular proteins. While kinases, responsible for phosphorylation, are well-characterized, phosphatases governing dephosphorylation remain less explored. Human kinases number approximately 518, whereas only 137 phosphatases have been identified.[4] Nevertheless, research underscores the critical roles phosphatases play in liver diseases and the development of HCC. The intricate molecular mechanisms involved make HCC one of the most life-threatening malignancies on a global scale. Consequently, there is an urgent need for prognostic biomarkers to predict outcomes and tailor individualized treatment strategies for HCC patients. While gene markers with predictive value have emerged with advancements in gene sequencing technology, their numbers are limited. To enhance HCC prognosis and patient care, the identification of additional biomarkers with higher prediction accuracy is imperative. In this study, we conducted a comprehensive proteomic analysis through CPTAC.

Initially, our analysis identified a total of 11,547 phosphorylation sites associated with 4,043 phosphoproteins. Notably, these sites were quantified in over 50% of the samples. Among them, a significant 9,994 phosphorylation sites exhibited marked differential expression. Specifically, 8,198 sites displayed significant upregulation, while 1,796 sites showed downregulation in tumor samples when compared to their corresponding nontumor counterparts. This distinction was established through a paired two-sided Student's t test, with Benjamini-Hochberg (BH) adjusted p-values < 0.05. Within this

https://doi.org/10.1021/acsomega.4c01496
ACS Omega 2024, 9, 26075−26096

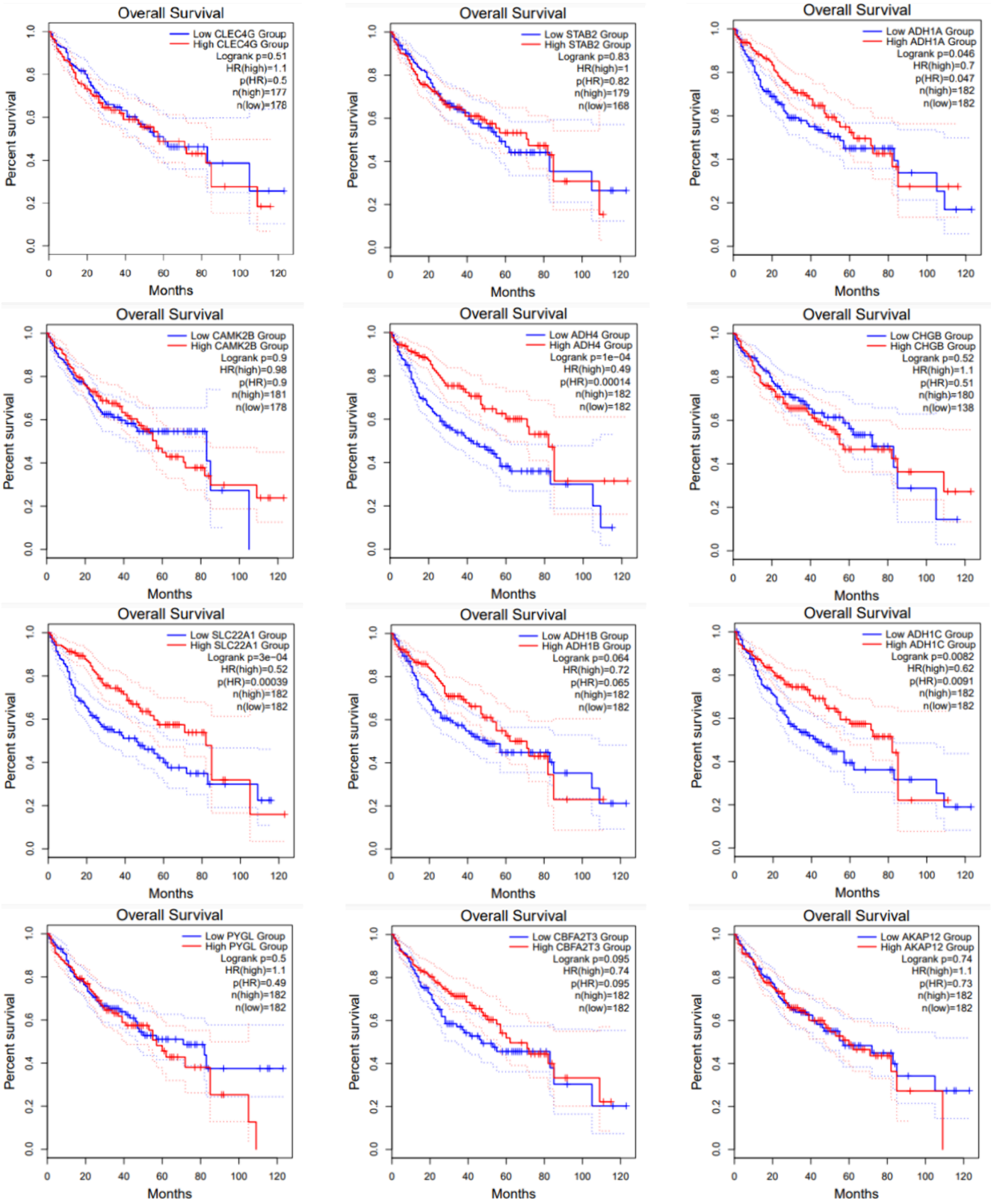

Figure 8. Kaplan−Meier OS plot analysis demonstrates that a group with elevated levels of 12 downregulated proteins experienced a worse prognosis than the group with lower levels ($P < 0.05$). Dashed lines represent the upper and lower confidence intervals.

data set, we focused on 19 phosphorylation sites, all demonstrating significant changes between samples (with *p*-values < 0.05). Our comprehensive analysis of these 12 proteins and their associated phosphosites highlighted a downregulation pattern in 12 unique genes. This observation prompts further exploration to better understand the functions of these proteins and their phosphorylation sites in the context of HCC. This study extensively explored downregulated genes and their

https://doi.org/10.1021/acsomega.4c01496
ACS Omega 2024, 9, 26075−26096

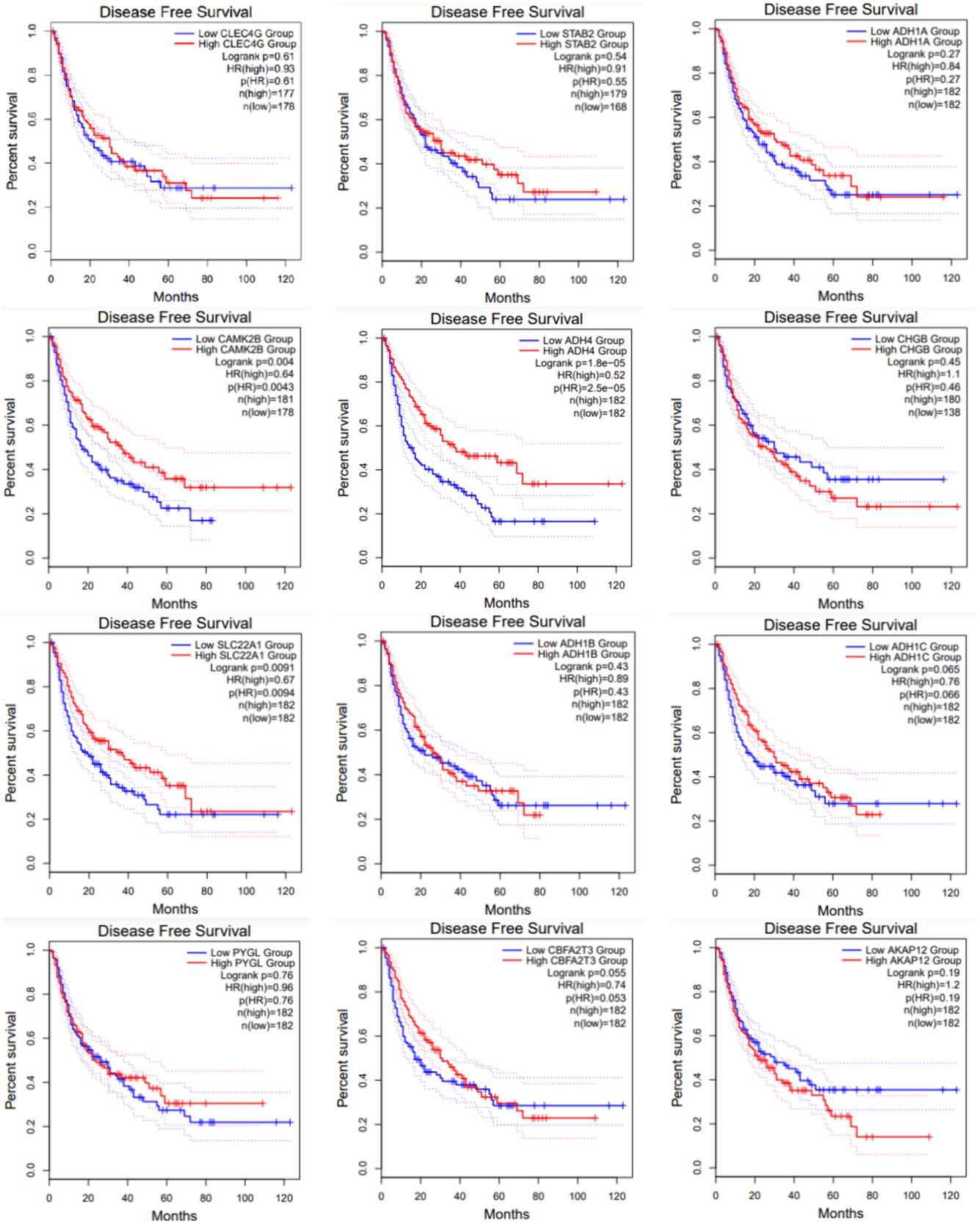

Figure 9. Kaplan−Meier disease free survival plot analysis demonstrates that a group with elevated levels of 12 proteins experienced a worse prognosis than the group with lower levels ($P < 0.05$). Dashed lines represent the upper and lower confidence intervals.

associated phosphorylation sites, such as CLEC4G, STAB2, ADH1A, ADH1B, CAMK2β, ADH4, CHGB, AKAP12, PYGL, ADH1C, CBFA2T3, and SLC22A1. Utilizing bioinformatics tools, we assessed gene expression levels and identified potential

https://doi.org/10.1021/acsomega.4c01496
ACS Omega 2024, 9, 26075−26096

Table 4. Five Common FDA Approved Drug Candidate Targeting SLC22A1, CAMK2B, and AHD1A

no.	gene	drug	approved
1	CAMK2B	Sorafenib	FDA
2	SLC22A1		
3	SLC22A1	Imatinib	FDA
5	ADH1A	Cytarabine	FDA
6	ADH1A	Fludarabine	FDA
7	ADH1A	Idarubicin	FDA
8	CAMK2B	Cediranib	Not
9	CAMK2B	Cenisertib	Not
10	CAMK2B	SNS-314	Not
4	CAMK2B	Linifanib	Not

therapeutic targets. Our aim was to determine the clinical relevance of these genes and assess their impact on HCC biology. The phosphopeptide enrichment strategy employed here yielded novel insights into phosphoproteins linked to liver cancer. This comprehensive analysis sheds light on the intricate signaling pathways mediated by phosphorylation in cancers, specifically within tumor cell lines.

Alcohol dehydrogenases (ADHs) play a critical role in ethanol metabolism, and increased alcohol consumption escalates the risk of liver cancer, primarily through cirrhosis development. Our ongoing research aims to unravel the multifaceted roles of ADH1A, ADH1B, ADH1C, and ADH4 in disease progression, investigating their potential as therapeutic targets. As we delve deeper into their functions, we seek to identify therapeutic opportunities not only in liver cancer but also in other cancer types. In our current study, our data revealed significant downregulation of phosphorylated ADH1A at S365 (log FC = −2.9; p-value = 1.9×10^{-36}), ADH1B at S109 (log FC = −2.8; p-value = 1.9×10^{-34}), ADH1C at S165 (log FC = −2.1; p-value = 5.5×10^{-61}), ADH4 at S278 (log FC = −2.7; p-value = 4.2×10^{-56}), and ADH4 at S330 (log FC = −2.1; p-value = 4.9×10^{-53}) compared to normal liver samples. Our GO enrichment analysis highlighted the contribution of ADHs to ethanol metabolism, including pathways such as ethanol metabolic, retinoid metabolic, and primary alcohol metabolic pathways. Moreover, KEGG pathways enrichment analysis indicated significant pathway enrichments, including tyrosine metabolism, fatty acid degradation, retinol metabolism, glycolysis/gluconeogenesis, drug metabolism-cytochrome P450, and metabolism of xenobiotics by cytochrome P450. Notably, our Kaplan−Meier analysis revealed that high expression levels of ADH1A, ADH1B, ADH1C, and ADH4 were associated with a favorable OS rate in HCC patients, serving as independent factors contributing to improved prognosis for both OS and DFS. Particularly, high expression of ADH4 was identified as an independent factor significantly associated with improved DFS ($p = 2.5 \times 10^{-5}$). The comprehension of ADH phosphorylation at specific sites S (365, 109, 165, 278, and 330) and its ensuing functional consequences carries promising therapeutic implications. Depending on its precise role in distinct cancer contexts, exploring the prospect of targeting ADHs or the associated signaling pathways as a therapeutic strategy holds potential. Our ongoing research aims to unravel the significance of ADHs in liver cancer and their potential as therapeutic targets.

Stabilin-2 (STAB2), also referred as FEEL-2, belongs to the highly conserved type I transmembrane proteins within the scavenger receptor family.[56] Previous investigations have highlighted STAB2 involvement in the proliferation and distant metastasis of melanoma cells, as well as lymph node metastasis in prostate and tongue cancers.[57] While STAB2 exhibits low expression levels in several human tissues, it is highly expressed in the noncontinuous sinusoidal endothelium of liver, spleen, lymph node, and bone marrow tissues.[58] Despite its known expression pattern, limited research has explored the role of STAB2 in HCC. Therefore, our study aimed to explore the correlation between STAB2 expression levels and HCC using multiple data sets. In our investigation, we successfully quantified the downregulation of phosphorylated STAB2 at S2497 (log FC = −3.5; p-value = 9.9×10^{-37}) in tumor patients compared to nontumor patients. These findings suggest that the phosphorylation status of STAB2 at S2497 may hold significant implications in HCC and could potentially serve as a protective factor, possibly related to hyaluronic acid (HA) clearance. Moreover, our functional enrichment analyses revealed STAB2 involvement in crucial biological processes, including mucopolysaccharide and glycosaminoglycan metabolic processes, glycosaminoglycan binding, fat digestion and absorption, regulation of cell substrate adhesion, and modulation of the apoptotic signaling pathway. Notably, PPI analysis highlighted significant interactions between STAB2 and pivotal hub genes in HCC, such as CD44 and APOB. A recent study emphasized the role of CD44 in HCC initiation, underscoring its ability to enhance growth factor signaling while inhibiting p53 function, a critical factor in HCC initiation.[59] Furthermore, our study utilized STAB2 mRNA expression data obtained from The Cancer Genome Atlas (TCGA) database. We processed the raw data through normalization and transformation procedures using RStudio software. Our Kaplan−Meier analysis revealed that high expression levels of STAB2 were associated with a favorable OS rate in HCC patients, serving as independent factors contributing to improved prognosis for both OS and DFS. The role of STAB2 in HCC has not been extensively studied and should be further investigated. Such research could prove to be highly valuable for the clinical diagnosis of HCC in the future.

CaMK2 (calcium/calmodulin-dependent protein kinase 2) is a multifunctional serine/threonine-protein kinase that plays a crucial role in various cellular processes. Its significance lies in mediating the Ca^{2+} signaling cascade. In recent studies, CAMK2 has been increasingly recognized for its involvement in cancer development. The critical involvement of CAMK2 in HCC progression has recently been documented. Initially, the potential impact of CAMK2 on liver cancer was indirectly evaluated through a straightforward experiment.[60] KN-62, identified as a pharmacological inhibitor of CAMK2, exhibited specific and effective suppression of protein synthesis and functional activity of hypoxia-inducible factor (HIF)-1α in hepatoma cells under hypoxic conditions. The quantitative proteomics analysis for the first time that identified p-sites of CAMK2β at S411, S454, and T341. These phosphopeptides exhibited varying abundances, with corresponding log FC values of −2.53, −2.73, and −2.73, respectively. Importantly, these p-sites are significantly downregulated with p-values of 3.77×10^{-52}, 3.4×10^{-21}, and 3.4×10^{-21}, respectively. Results from this experiment showed that CAMK2 (mainly the β isoform) plays a significant role in the growth and development of liver cancer. The phosphorylation of CAMK2 at T286 for the α isoform or at T287 for the β, γ, and δ isoforms has been established as a biomarker for CAMK2 activation.[61] The BP, CC, MF, and KEGG pathway enrichment analyses of CAMK2β

https://doi.org/10.1021/acsomega.4c01496
ACS Omega 2024, 9, 26075−26096

ADH1A (Non-tumor) Staining: Medium Intensity: Moderate Quantity: >75% Location: Cytoplasmic/membranous	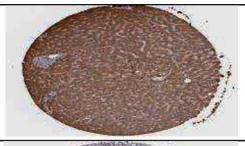		**ADH1A** (Tumor) Staining: High Intensity: Strong Quantity: >75% Location: Cytoplasmic/membranous
CAMK2B (Non-tumor) Staining: Not detected Intensity: Negative Quantity: Negative Location: None	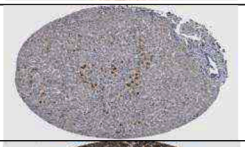	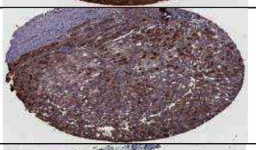	**CAMK2B** (Tumor) Staining: High Intensity: Strong Quantity: 75%-25% Location: Cytoplasmic/membranous
ADH4 (Non-tumor) Staining: Medium Intensity: Moderate Quantity: 75%-25% Location: Cytoplasmic/membranous	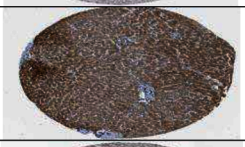	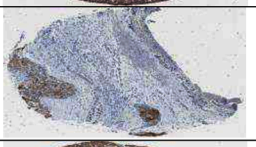	**ADH4** (Tumor) Staining: Medium Intensity: Moderate Quantity: 75%-25% Location: Cytoplasmic/membranous
STAB2 (Non-tumor) Staining: Not detected Intensity: Negative Quantity: Negative Location: None		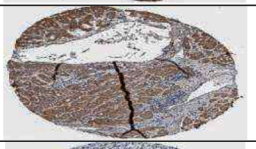	**STAB2** (Tumor) Staining: Medium Intensity: Moderate Quantity: >75% Location: Cytoplasmic/membranous
CLEC4G (Non-tumor) Staining: Not detected Intensity: Weak Quantity: <25% Location: Cytoplasmic/membranous	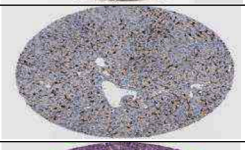	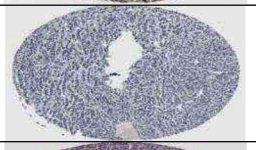	**CLEC4G** (Tumor) Staining: Not detected Intensity: Negative Quantity: None Location: None
CHGB (Non-tumor) Staining: Not detected Intensity: Negative Quantity: None Location: None	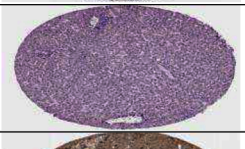	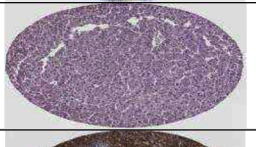	**CHGB** (Tumor) Staining: Not detected Intensity: Negative Quantity: None Location: None
SLC22A1 (Non-tumor) Staining: Medium Intensity: Moderate Quantity: 75%-25% Location: Cytoplasmic/membranous	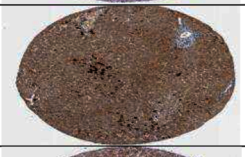		**SLC22A1** (Tumor) Staining: Medium Intensity: Moderate Quantity: 75%-25% Location: Cytoplasmic/membranous
ADH1B (Non-tumor) Staining: Medium Intensity: Moderate Quantity: 75%-25% Location: Cytoplasmic/membranous	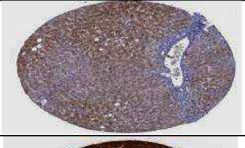	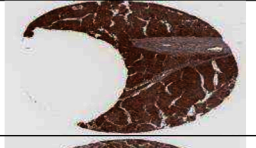	**ADH1B** (Tumor) Staining: High Intensity: Strong Quantity: >75% Location: Cytoplasmic/membranous
ADH1C (Non-tumor) Staining: High Intensity: Negative Quantity: 75%-25% Location: Cytoplasmic/membranous	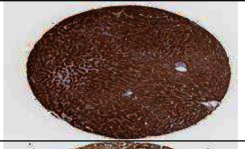		**ADH1C** (Tumor) Staining: High Intensity: Strong Quantity: 75%-25% Location: Cytoplasmic/membranous
PYGL (Non-tumor) Staining: High Intensity: Strong Quantity: 75%-25% Location: Cytoplasmic/membranous	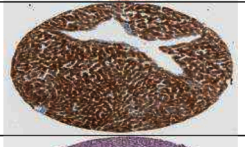	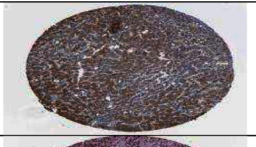	**PYGL** (Tumor) Staining: Medium Intensity: Moderate Quantity: >75% Location: Cytoplasmic/membranous
CBFA2T3 (Non-tumor) Staining: Not detected Intensity: Negative Quantity: None Location: None	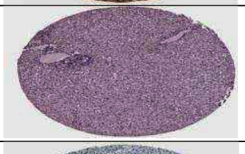	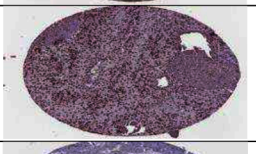	**CBFA2T3** (Tumor) Staining: High Intensity: Moderate Quantity: >75% Location: Cytoplasmic/membranous
AKAP12 (Non-tumor) Staining: Not detected Intensity: Negative Quantity: None Location: None	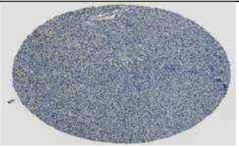	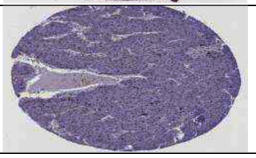	**AKAP12** (Non-tumor) Staining: Not detected Intensity: Negative Quantity: None Location: None

Figure 10. Immunohistochemistry images of 12 hub genes in normal liver and HCC tissues derived from the Human Protein Atlas (HPA) database (http://www.proteinatlas.org/).

were conducted, revealing significant enrichment in these categories ($p < 0.05$). The BP analysis highlighted the involvement of protein in metabolic processes. In the CC analysis, the proteins were categorized into extracellular exosome and various cellular compartments. MF analysis demonstrated that the majority of detected p-sites exhibit

https://doi.org/10.1021/acsomega.4c01496
ACS Omega 2024, 9, 26075−26096

molecule binding and structural activity. Moreover, the KEGG pathway enrichment analysis highlighted pathways such as metabolic pathways and glucagon signaling pathway as significantly associated with CAMK2β. Our Kaplan−Meier analysis showed a correlation between high levels of CAMK2β expression and a favorable OS rate. Moreover, high CAMK2β expression significantly ($p = 0.004$) correlated with a good DFS. It is important to note the limited research focused on CAMK2β in HCC patients, emphasizing the urgent need for comprehensive data collection to elucidate crucial insights into this protein's role.

CLEC4G (C-type lectin domain family 4 member G) also recognized as liver and lymph node sinusoidal endothelial cell C-type lectin (LSECtin), belongs to subgroup II of the C-type (Ca^{2+}-dependent) lectin superfamily. CLEC4G/LSECtin exhibits binding affinity toward mannose, GlcNAc, and fucose in a Ca^{2+}-dependent manner. Additionally, this protein possesses the capability to bind to surface glycoproteins found on enveloped viruses. Notably, CLEC4G/LSECtin has been observed to interact with the surface glycoproteins of severe acute respiratory syndrome (SARS) coronavirus and the Ebola virus. Specifically, it has been described that LSECtin-mediated infection of cells by the Ebola virus occurs through this interaction. Moreover, our findings regarding CLEC4G, and its phosphorylation site (S12) have demonstrated significant downregulation with a log fold change of (log FC = −4.5; p-value = 7.71×10^{-26}). The MF analysis revealed that CLEC4G exhibits mannose binding, monosaccharide binding, and polysaccharide binding properties. To our knowledge, we were the first to report the downregulation of CLEC4G in HCC compared to normal tissues, suggesting a potential role of CLEC4G in angiogenesis. In our study, we found that HCC patients expressing low levels of CLEC4G exhibited correlations with both a poor OS rate and disease-free survival. Furthermore, we observed higher expression of both CLEC4G mRNA and protein levels in normal liver tissues ($p < 0.01$). These findings suggest that CLEC4G could serve as a reliable diagnostic marker for HCC.

The **SLC22A1** gene has been extensively studied in various types of tissues and tumor cell lines. However, information regarding its presence and role in human malignancies is limited. Our recent findings revealed a notable downregulation of SLC22A1 in human HCC. Additionally, we reported that reduced levels of OCT1 mRNA in HCC correlate with an advanced tumor stage and poorer patient survival. We developed a risk score model and constructed a nomogram that utilizes prognosis-associated genes in conjunction with clinical factors to predict the prognosis of HCC. Furthermore, our investigation identified phosphorylation sites on SLC22A1 at S321 and T541. Interestingly, we observed a significant downregulation of phosphorylation at these sites, with log FC values of −2.1 (p-value = 5.73×10^{-33}) and −2.3 (p-value = 4.77×10^{-25}), respectively. The MF analysis unveiled various activities attributed to SLC22A1, including transmembrane transporter activity, sodium chloride symporter activity, neurotransmitter transmembrane transporter activity, and organic cation transmembrane transporter activity. Additionally, The GO analysis revealed enrichment in terms such as chemical carcinogenesis and drug metabolism cytochrome P450. These findings suggest their potential significance in unraveling the mechanisms underlying hepatocarcinogenesis. Significantly, our Kaplan−Meier analysis highlighted that elevated expression levels of SLC22A1 were markedly associated with a favorable OS rate ($p = 0.0004$) as well as DFS ($p = 0.0094$) among patients with HCC. These findings highlight that high expression of SLC22A1 correlates to an improved prognosis for both OS and DFS in HCC patients. Moreover, SLC22A1 demonstrates a pivotal role in modulating cell proliferation, potentially serving as an indicator for recurrence prediction after surgical intervention in HCC cases. These revelations position SLC22A1 as a promising candidate for both prognostic assessment and as a target for therapeutic intervention in HCC. Further investigations are imperative to delve deeper into the precise mechanisms and regulatory pathways through which SLC22A1 influences the progression and behavior of HCC.

In this study, we successfully quantified the phosphorylation levels of CHGB at S130, S225, and S391, revealing significant downregulation with log FC values of −2.37 (p-value = 2.37×10^{-49}), −2.45 (p-value = 5.28×10^{-38}), and −2.53 (p-value = 4.16×10^{-44}), respectively, in tumor patients compared to nontumor patients. The phosphorylation of these specific serine residues may significantly impact CHGB function and its involvement in cellular processes in HCC. Our ongoing research aims to elucidate CHGB specific functions, clinical relevance, and potential as a therapeutic target in HCC due to limited existing research on this protein. Additionally, our analysis of the independent validation data set from the CPTAC data set revealed an increase in OS for the low-risk group compared to the high-risk group. Notably, these results were consistent with our findings in the TCGA data set for both OS and DFS. However, the clinical implications of this finding remain unclear, and the consequences of CHGB inhibition on the effectiveness of targeted therapies have not been fully elucidated.

The role of **PYGL** in cancer, particularly in HCC, remains an understudied area requiring further investigation. In this study, we analyzed PYGL expression levels, revealing higher expression in tumor tissues, particularly in HCC, compared to normal tissues. High PYGL expression (HR = 1.1; $p = 0.52$) showed a trend in predicting poor prognosis among HCC patients. Moreover, upon clinical data analysis, elevated PYGL levels were observed in late-stage HCC patients, potentially indicating a correlation between PYGL and disease progression. Further investigation is necessary to comprehensively assess the relationship between PYGL expression and disease advancement in late-stage HCC. Notably, our investigation identified a significantly downregulated phosphorylation site on PYGL at S605, with log FC values of −2.43 and a p-value of 6.82×10^{-70}. These findings suggest a potential substantial role of PYGL in the development and progression of HCC. This insight could offer valuable directions for therapeutic targets and avenues for further research, thereby enhancing our understanding of the molecular mechanisms underlying hepatocellular carcinoma. Furthermore, the analysis highlighted PYGL involvement in metabolic processes in the biological process (BP) category. In cellular component (CC) analysis, proteins were categorized into cytosol, cytoplasmic vesicles, and various cellular compartments. MF analysis revealed that most detected phosphorylation sites exhibit bindings such as monosaccharide, vitamin, glucose, AMP, and carbohydrate. Additionally, the KEGG pathway enrichment analysis underscored pathways like metabolic pathways and the glucagon signaling pathway, significantly associated with PYGL. Collectively, our study suggests that glycogen metabolism and the involvement of GP play crucial roles in the progression of HCC, presenting potential novel therapeutic targets for HCC therapy. The prospect of combining standard antiangiogenic therapy with antimetabolism therapy

https://doi.org/10.1021/acsomega.4c01496
ACS Omega 2024, 9, 26075−26096

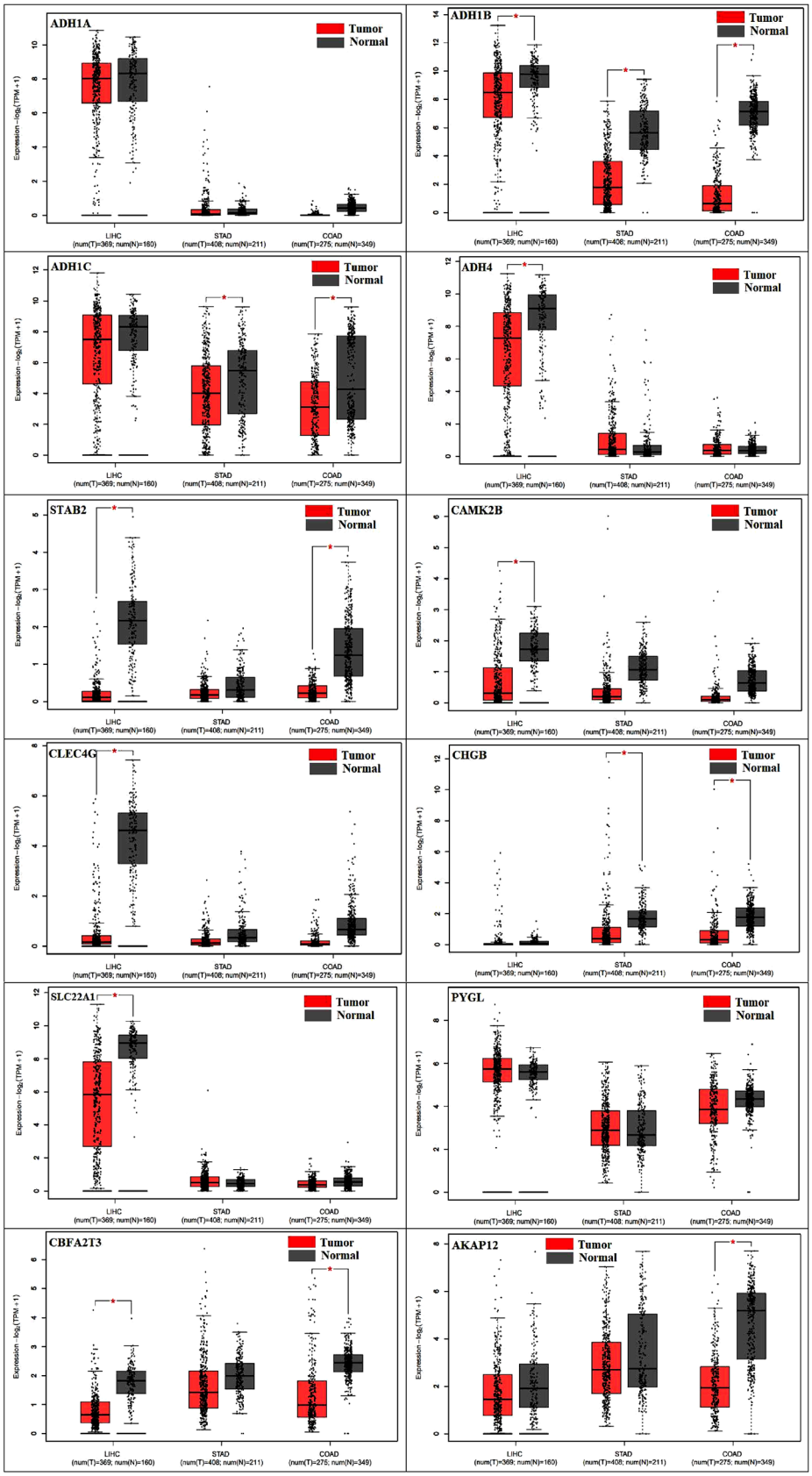

Figure 11. Expression levels of 12 genes in HCC, comparing normal liver tissues (depicted by a black box) with HCC (indicated by a red box). These findings were obtained from the GEPIA online tool (* $p < 0.01$; tumor vs normal).

https://doi.org/10.1021/acsomega.4c01496
ACS Omega 2024, 9, 26075−26096

emerges as a promising strategy to enhance the treatment effectiveness for HCC.

A-kinase anchor protein 12 (AKAP12) belongs to the A-kinase anchoring protein family, functioning as a scaffold protein in signal transduction pathways. It plays an antitumor role in various human cancers, including breast cancer, esophageal neoplastic progression, myeloid malignancies, colorectal cancer, gastric cancer, and HCC.[42] In HCC tissues, AKAP12 mRNA expression was found to be downregulated, showing a negative correlation with the level of miR-1251−5p.[62] Subsequent in vitro experiments confirmed that miR-1251−5p directly targets and negatively regulates AKAP12 expression. In our study, we noted a downregulation of AKAP12 expression in tumor patients compared to nontumor patients, and this downregulation was correlated with a poor prognosis. Additionally, we observed that AKAP12 undergoes phosphorylation at S286, and this phosphorylation was significantly downregulated, with a log FC value of −2.25 and a p-value of 7.8×10^{-37}. Previous studies have documented the downregulation of AKAP12 in human HCC, attributing it to promoter hypermethylation, chromosomal deletion, and specific microRNAs. To deepen our understanding of AKAP12 functions and underlying mechanisms in HCC progression, further research is necessary. Our GO enrichment analysis revealed several significant contributions of AKAP12, including calmodulin binding and adenylate cyclase binding. Additionally, the KEGG pathways enrichment analysis highlighted several pathways significantly associated with AKAP12, such as tyrosine metabolism, fatty acid degradation, retinol metabolism, glycolysis/gluconeogenesis, drug metabolism-cytochrome P450, and metabolism of xenobiotics by cytochrome P450. These findings from our study suggest a potential novel mechanism associated with AKAP12-dependent inhibition.

Our recent study meticulously examined and successfully quantified the phosphorylation sites of CBFA2T3 at S510 and S564. The findings revealed a notable downregulated pattern with log FC values of −2.20 (p-value = 4.1×10^{-24}) and −2.26 (p-value = 6.5×10^{-43}) for these phosphorylation markers in tumor tissues compared to nontumor tissues. This observation is crucial considering that cancer, including HCC, is characterized by the aberrant dysregulation of signaling cascades and cellular processes. Phosphorylation events affecting proteins can significantly contribute to the perturbation of these pathways, potentially fostering the uncontrolled proliferation, survival, or metastasis of cancer cells. Additionally, our Kaplan−Meier analysis unveiled a noteworthy association between high expression levels of CBFA2T3 and a favorable OS rate in HCC patients. These findings indicate that CBFA2T3 expression serves as an independent factor contributing to improved prognosis for both OS and DFS in HCC. However, the clinical implications of this finding remain unclear, and a comprehensive understanding of the consequences of CBFA2T3 inhibition on the effectiveness of targeted therapies has yet to be fully elucidated.

Maintaining the equilibrium between phosphorylation and dephosphorylation is pivotal for cellular function. Dysregulation of these processes, controlled by protein kinases and phosphatases, can contribute to disease.[4] In cancer research, identifying early biomarkers for HCC is challenging due to varied influences on molecular changes. Advanced proteomic and genomic techniques aid in deciphering potential HCC biomarkers. Our study pinpointed CLEC4G, STAB2, ADH1A, ADH1B, CAMK2β, CBFA2T3, ADH4, CHGB, PYGL, ADH1C, and SLC22A1 genes, driving alterations in the liver microenvironment and HCC development. These genes impact liver cells signaling pathways, influencing HCC progression by modulating the liver microenvironment constituents. This emphasizes their potential as therapeutic targets. Ongoing research seeks to unravel these genes functional dimensions, aiming to revolutionize HCC management through innovative diagnostics and targeted therapies. We performed a comprehensive analysis of KEGG pathways and GO terms associated with the phosphorylated proteins. Notably, enriched KEGG pathways encompassed tyrosine metabolism, fatty acid degradation, retinol metabolism, alcohol liver disease, drug metabolism-cytochrome P450, and pyruvate metabolism. Our GO analysis highlighted significant enrichments in BP, CC, and MF. Specifically, the 12 significant genes were found to play key roles in vital biological processes.

We created a PPI network using the STRING database, identifying 19 hub genes, among which 12 key genes, notably CLEC4G, STAB2, ADH1A, ADH1B, CAMK2β, ADH4, CHGB, PYGL, ADH1C, CBFA2T3, AKAP12, and SLC22A1, exhibited significant relevance. Elevated expression of these key genes correlated strongly with increased survival in HCC patients, validated by survival analysis and gene/protein-level expression assessments. These genes primarily participate in pathways like tyrosine metabolism, fatty acid degradation, retinol metabolism, and glucagon signaling pathways. Validation through TCGA database comparison of gene expression between tumor and normal tissues, alongside immunohistochemical analysis and screening for potential drugs for HCC, augmented the credibility and depth of our study, which integrates data from CPTAC, TCGA, and RTCGA databases.

To comprehensively understand the roles of specific genes in HCC, we conducted an expression analysis utilizing TCGA data, focusing on the top 12 significantly implicated genes. Our aim was to compare their expression levels across various cancer types, particularly STAD (stomach adenocarcinoma), COAD (colon adenocarcinoma), and LIHC (liver hepatocellular carcinoma), due to their liver metastatic tendencies. Analyzing these genes contributes significantly to distinguishing primary liver cancer (HCC) from metastatic liver lesions. This exploration of distinct gene expression patterns in different cancers aims to unveil potential diagnostic markers for accurately differentiating primary and metastatic liver malignancies. The results, depicted in Figure 11 and analyzed using GEPIA 2 software, revealed lower expression levels in tumor samples compared to nontumor samples across these cancer types. We conducted Student's t tests to calculate p-values for expression differences of genes between normal controls and cancer samples, setting threshold parameters for p-values and fold change at 0.01 and 2, respectively. Our analysis consistently showed decreased expression of specific genes in tumor tissues compared to normal tissues across the studied cancers. In STAD, ADH1B, ADH1C, and CHGB, and exhibited significantly lower expression levels. COAD samples displayed notable decreases in ADH1B, ADH1C, STAB2, CHGB, CBFA2T3, and AKAP12 expression. In LIHC, ADH1B, ADH4, STAB2, CAMK2β, CLEC4G, SLC22A1, and CBFA2T3 were notably downregulated. Our findings suggest that ADH1B, ADH1C, STAB2, CAMK2β, ADH4, CHGB, CLEC4G, and CBFA2T3 are promising diagnostic biomarkers, being significantly downregulated across STAD, COAD, and LIHC.

TCGA serves as a pivotal resource encompassing genomic data from more than 2000 primary neoplasms and their

https://doi.org/10.1021/acsomega.4c01496
ACS Omega 2024, 9, 26075−26096

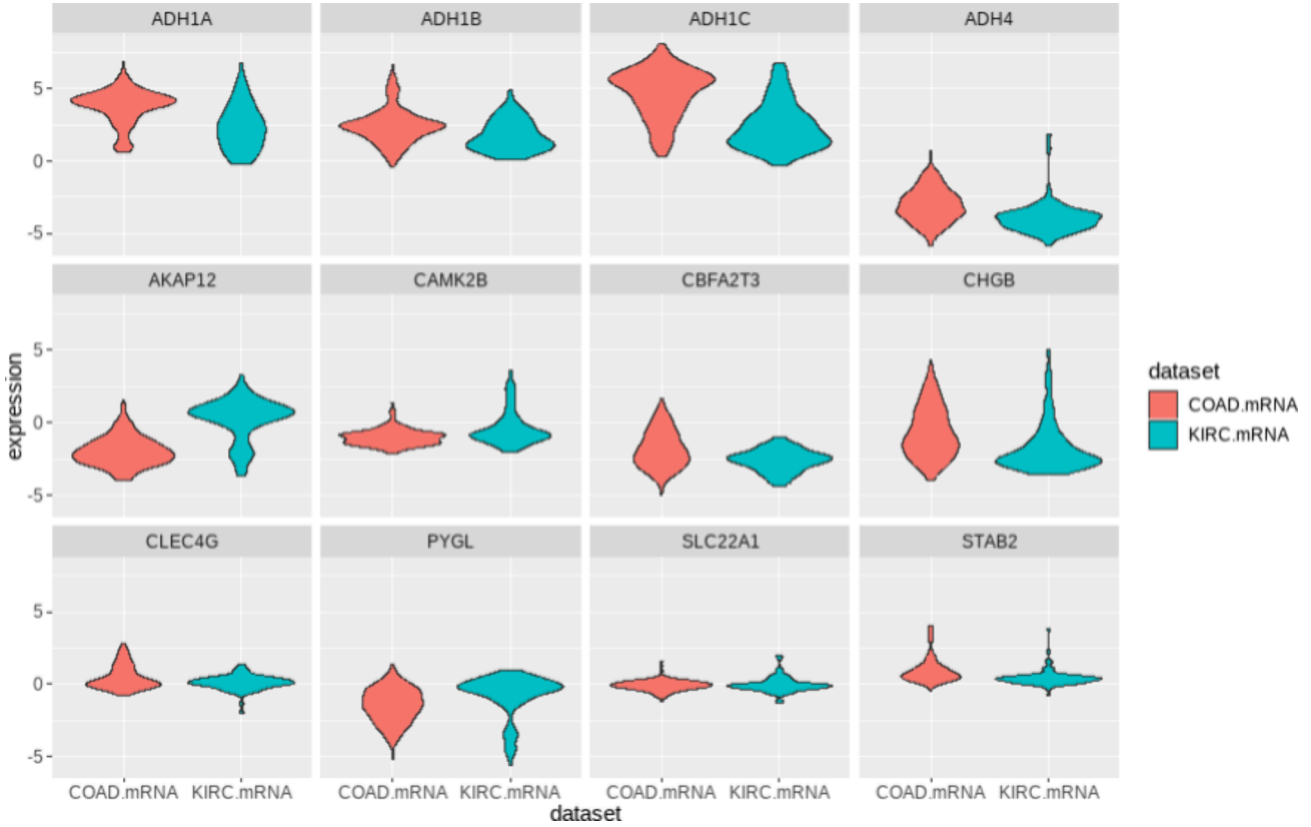

Figure 12. mRNA expression levels of the 12 genes within HCC as compared between COAD mRNA and KIRC mRNA data sets, derived from the RTCGA package in the RStudio program.

corresponding normal samples, offering extensive insights into cancer genomics (https://cancergenome.nih.gov/). For our investigation, we accessed mRNA expression profiles and associated clinical details via the TCGA database, specifically utilizing the RTCGA package within the RStudio software to procure the data. Our focus lay on data sets COAD mRNA and kidney renal clear cell carcinoma (KIRC) mRNA. The data analysis conducted using RStudio produced results outlined in Figure 12 and summarized in Table S4 (mRNA Expression). The comparison aims to highlight potential differential gene expression patterns across different cancer types, providing insights into the distinct mRNA expression profiles of these genes in HCC in contrast to other malignancies such as COAD and KIRC. The integral role of these genes in liver cancer cannot be understated. As our comprehension of the intricate molecular mechanisms driving cancer progression, particularly in the context of liver cancer, evolves, it holds promise for developing targeted therapies capable of specifically addressing dysregulation within these gene families and their phosphorylation sites.

The analysis did not reveal a statistically significant difference in OS between groups (p-value = 0.56). However, our multivariable Cox regression analysis uncovered several significant predictors of recurrence postliver resection in our patient cohort. Established clinical indicators such as tumor size, number, and vascular invasion were validated as predictors of poor outcomes. Additionally, higher expression levels of certain genes emerged as significant predictors of recurrence, with HR > 1.0 and $p < 0.05$. Notably, genes displaying increased expression specifically ADH1C, ADH4, and SLC22A1 showed a significant correlation with OS in HCC patients, while ADH4, SLC22A1, CAMK2β, and CBFA2T3 correlated significantly with shorter DFS. These findings highlight the potential pivotal roles of these genes in HCC prognosis. An intriguing aspect lies in the therapeutic implications, considering that inhibitors targeting ADH1C, ADH4, SLC22A1, CAMK2β, and CBFA2T3 have not undergone extensive study, either as standalone treatments or in combination with established anticancer agents. Exploring these avenues could offer promising strategies to augment cancer treatment efficacy and mitigate HCC progression. Continued investigations in this domain hold the potential to revolutionize the management and treatment approaches for liver cancer patients. In summary, our research provides novel insights into the phosphoproteomic landscape of in HCC, contributes valuable information to the field, and proposes a potential biomarker combination for enhanced diagnostic and prognostic capabilities in HCC.

CONCLUSION

We conducted a ground-breaking analysis of the phosphoproteome and proteomic profile associated with HCC. This investigation pioneers the unveiling of a novel protein signature through integrated analysis and PPI assessments. The observed dysregulation of CLEC4G, STAB2, ADH1A, ADH1B, CAMK2β, ADH4, CHGB, PYGL, ADH1C, CBFA2T3, AKAP12, and SLC22A1 indicates distinct structural variations and potential migratory behaviors between tumor and paired nontumor tissues. Moreover, the significant alterations in phosphorylation sites potentially hold biological relevance for HCC malignancy. These findings serve as a valuable resource for the broader scientific community engaged in HCC research, offering promising avenues for the development of new drugs. Additionally, a group of drug molecules was scrutinized,

https://doi.org/10.1021/acsomega.4c01496
ACS Omega 2024, 9, 26075−26096

potentially exploitable for HCC treatments. Our comprehensive survival analysis, considering multiple intersecting markers, sheds new light on the complex interactions among these markers in predicting cancer patient outcomes. The results highlight the association of high gene expression in HCC with poor prognosis. KEGG and GO pathway analyses suggest that these genes may impact liver cancer through various targets and pathways, ultimately promoting HCC development and progression. Notably, our study identifies significantly down-regulated levels of ADH1B, STAB2, CLEC4G, ADH4, SLC22A1, STAB2, CAMK2β, and CBFA2T3, presenting promising avenues for further exploration. This substantial expression could serve as potent diagnostic and prognostic markers, potentially enhancing the effectiveness of HCC cancer treatment, reducing mortality rates, and improved accuracy in patient assessment. In our future plans, we aspire to design, repurpose, and discover drug molecules targeting ADH4, STAB2, and SLC22A1, CLEC4G, and CAMK2β. Furthermore, our agenda includes characterizing previously unidentified proteins to comprehend their roles in HCC.

■ ASSOCIATED CONTENT

Data Availability Statement

The data sets used and analyzed during the current study are available upon reasonable request from the corresponding author. Due to the ongoing experiment's requirements in the later stages, the data will be released at this time.

Supporting Information

The Supporting Information is available free of charge at https://pubs.acs.org/doi/10.1021/acsomega.4c01496.

> Detailed information on phosphosites, peptide, gene, and log ratios for all patients included in the study, comprehensive information on the demographic and clinical characteristics of patients diagnosed with HCC who were included in the study, providing essential patient-related data to contextualize the findings, comprehensive overview of the GO analysis conducted in this study using GSEA, mRNA expression analysis of two crucial data sets, COAD and KIRC (XLSX)

■ AUTHOR INFORMATION

Corresponding Author

Aktham Mestareehi − *Department of Pharmaceutical Sciences, Faculty of Pharmacy, Isra University, Amman 11622, Jordan; School of Medicine, The Ohio State University, Columbus, Ohio 43202, United States; Department of Pharmaceutical Sciences, School of Pharmacy and Health Sciences, Wayne State University, Detroit, Michigan 48201, United States;* orcid.org/0000-0002-1478-6310; Email: mestareehi.1@osu.edu

Complete contact information is available at: https://pubs.acs.org/10.1021/acsomega.4c01496

Author Contributions

The manuscript was written by the author, who provided his consent and approval for the final version. A.M. contributed to the methodology, formal analysis, and data curation. Additionally, A.M. was responsible for drafting the original manuscript, contributed to manuscript review and editing, supervised the project, administered the research, and acquired funding.

Notes

The data used in our study were exclusively sourced from the CPTAC, TCGA, and HPA data sets and were not derived from our own clinical samples. It is important to emphasize that our current study received ethical approval and consent from the ethics committee.

The author declares no competing financial interest.

■ ACKNOWLEDGMENTS

This research did not receive any specific grant from funding agencies in the public, commercial, or not-for-profit sectors. We sincerely thank the TCGA, GEPIA, HPA, Kaplan−Meier Plotter, and TIMER platforms and the authors who uploaded the original data. In addition, thanks to all the authors who contributed to this article and to the publisher for supporting this article.

■ REFERENCES

(1) Sartorius, K.; Sartorius, B.; Aldous, C.; Govender, P.; Madiba, T. Global and country underestimation of hepatocellular carcinoma (HCC) in 2012 and its implications. *Cancer epidemiology* **2015**, *39*, 284−290.

(2) Falade-Nwulia, O.; et al. Oral direct-acting agent therapy for hepatitis C virus infection: a systematic review. *Annals of internal medicine* **2017**, *166*, 637−648.

(3) Razavi-Shearer, D.; et al. Global prevalence, treatment, and prevention of hepatitis B virus infection in 2016: a modelling study. *lancet Gastroenterology & hepatology* **2018**, *3*, 383−403.

(4) Mestareehi, A.; Zhang, X.; Seyoum, B.; Msallaty, Z.; Mallisho, A.; Burghardt, K. J.; Kowluru, A.; Yi, Z. Metformin Increases Protein Phosphatase 2A Activity in Primary Human Skeletal Muscle Cells Derived from Lean Healthy Participants. *J. Diabetes Res.* **2021**, *2021*, No. 9979234.

(5) Sheppeck, J. E., 2nd; Gauss, C. M.; Chamberlin, A. R. Inhibition of the Ser-Thr phosphatases PP1 and PP2A by naturally occurring toxins. *Bioorganic & medicinal chemistry* **1997**, *5*, 1739−1750.

(6) Ng, C. K. Y.; et al. Integrative proteogenomic characterization of hepatocellular carcinoma across etiologies and stages. *Nat. Commun.* **2022**, *13*, 2436.

(7) Edenberg, H. J.; McClintick, J. N. Alcohol dehydrogenases, aldehyde dehydrogenases, and alcohol use disorders: a critical review. *Alcoholism: Clinical and Experimental Research* **2018**, *42*, 2281−2297.

(8) Hashibe, M.; et al. Multiple ADH genes are associated with upper aerodigestive cancers. *Nature genetics* **2008**, *40*, 707−709.

(9) Abe, H.; et al. Aldehyde dehydrogenase 2 polymorphism for development to hepatocellular carcinoma in E ast A sian alcoholic liver cirrhosis. *Journal of Gastroenterology and Hepatology* **2015**, *30*, 1376−1383.

(10) Homann, N.; et al. Alcohol dehydrogenase 1C* 1 allele is a genetic marker for alcohol-associated cancer in heavy drinkers. *International journal of cancer* **2006**, *118*, 1998−2002.

(11) Wang, P.; Zhang, L.; Huang, C.; Huang, P.; Zhang, J. Distinct prognostic values of alcohol dehydrogenase family members for non-small cell lung cancer. *Med. Sci. Monit.* **2018**, *24*, 3578.

(12) Takeuchi, O.; Akira, S. Pattern recognition receptors and inflammation. *Cell* **2010**, *140*, 805−820.

(13) Hoober, J. K.; van Vliet, S. J.; Dudziak, D.; Eggink, L. L. Editorial: Sentinel CLECs at Immunological Decision Nodes. *Front. Immunol.* **2020**, *11*, 2066.

(14) Yu, W.; Ma, Y.; Ochoa, A. C.; Shankar, S.; Srivastava, R. K. Cellular transformation of human mammary epithelial cells by SATB2. *Stem cell research* **2017**, *19*, 139−147.

(15) Notani, D.; et al. Global regulator SATB1 recruits β-catenin and regulates TH2 differentiation in Wnt-dependent manner. *PLoS biology* **2010**, *8*, No. e1000296.

(16) Britanova, O.; et al. Satb2 is a postmitotic determinant for upper-layer neuron specification in the neocortex. *Neuron* **2008**, *57*, 378−392.

(17) Sankararaman, S.; Yanamandra, K.; Napper, D.; Caldito, G.; Dhanireddy, R. The prevalence of platelet activating factor acetylhydrolase single nucleotide polymorphisms in relationship to necrotizing enterocolitis in Northwest Louisiana infants. *SpringerPlus* **2013**, *2*, 1−6.
(18) Yu, W.; Ma, Y.; Shankar, S.; Srivastava, R. K. Chronic ethanol exposure of human pancreatic normal ductal epithelial cells induces cancer stem cell phenotype through SATB2. *Journal of cellular and molecular medicine* **2018**, *22*, 3920−3928.
(19) Erondu, N. E.; Kennedy, M. B. Regional distribution of type II Ca^{2+}/calmodulin-dependent protein kinase in rat brain. *J. Neurosci.* **1985**, *5*, 3270−3277.
(20) Sanhueza, M.; Lisman, J. The CaMKII/NMDAR complex as a molecular memory. *Molecular brain* **2013**, *6*, 10.
(21) Hell, J. W. CaMKII: claiming center stage in postsynaptic function and organization. *Neuron* **2014**, *81*, 249−265.
(22) Borgesius, N. Z.; et al. βCaMKII plays a nonenzymatic role in hippocampal synaptic plasticity and learning by targeting αCaMKII to synapses. *J. Neurosci.* **2011**, *31*, 10141−10148.
(23) Nagasaki, N.; Hirano, T.; Kawaguchi, S. y. Opposite regulation of inhibitory synaptic plasticity by α and β subunits of Ca^{2+}/calmodulin-dependent protein kinase II. *Journal of physiology* **2014**, *592*, 4891−4909.
(24) van Woerden, G. M.; et al. βCaMKII controls the direction of plasticity at parallel fiber-Purkinje cell synapses. *Nature neuroscience* **2009**, *12*, 823−825.
(25) Zhou, M.; et al. Effective lock-in strategy for proteomic analysis of corona complexes bound to amino-free ligands of gold nanoparticles. *Nanoscale* **2018**, *10*, 12413−12423.
(26) Steiner, H.-J.; Schmid, K.; Fischer-Colbrie, R.; Sperk, G.; Winkler, H. Co-localization of chromogranin A and B, secretogranin II and neuropeptide Y in chromaffin granules of rat adrenal medulla studied by electron microscopic immunocytochemistry. *Histochemistry* **1989**, *91*, 473−477.
(27) Lin, Z.; Li, Y.; Hang, Y.; Wang, C.; Liu, B.; Li, J.; Yin, L.; Jiang, X.; Du, X.; Qiao, Z.; et al. Tuning the Size of Large Dense-Core Vesicles and Quantal Neurotransmitter Release via Secretogranin II Liquid-Liquid Phase Separation. *Adv. Sci.* **2022**, *9*, No. 2202263.
(28) Bearrows, S. C.; Bauchle, C. J.; Becker, M.; Haldeman, J. M.; Swaminathan, S.; Stephens, S. B. Chromogranin B regulates early-stage insulin granule trafficking from the Golgi in pancreatic islet β-cells. *J. Cell Sci.* **2019**, *132*, No. jcs231373.
(29) Dominguez, N.; van Weering, J. R.; Borges, R.; Toonen, R. F.; Verhage, M. Dense-core vesicle biogenesis and exocytosis in neurons lacking chromogranins A and B. *Journal of Neurochemistry* **2018**, *144*, 241−254.
(30) Bartolomucci, A.; et al. The extended granin family: structure, function, and biomedical implications. *Endocrine reviews* **2011**, *32*, 755−797.
(31) Benedum, U. M.; et al. The primary structure of bovine chromogranin A: a representative of a class of acidic secretory proteins common to a variety of peptidergic cells. *EMBO journal* **1986**, *5*, 1495−1502.
(32) Yoo, S. H. Purification and pH-dependent secretory vesicle membrane binding of chromogranin B. *Biochemistry* **1995**, *34*, 8680−8686.
(33) Pimplikar, S.; Huttner, W. Chromogranin B (secretogranin I), a secretory protein of the regulated pathway, is also present in a tightly membrane-associated form in PC12 cells. *J. Biol. Chem.* **1992**, *267*, 4110−4118.
(34) Portela-Gomes, G. M.; Grimelius, L.; Wilander, E.; Stridsberg, M. Granins and granin-related peptides in neuroendocrine tumours. *Regulatory peptides* **2010**, *165*, 12−20.
(35) Warburg, O. On the origin of cancer cells. *Science* **1956**, *123*, 309−314.
(36) Praly, J.-P.; Vidal, S. Inhibition of glycogen phosphorylase in the context of type 2 diabetes, with focus on recent inhibitors bound at the active site. *Mini reviews in medicinal chemistry* **2010**, *10*, 1102−1126.
(37) Agius, L. Role of glycogen phosphorylase in liver glycogen metabolism. *Molecular aspects of medicine* **2015**, *46*, 34−45.
(38) Favaro, E.; et al. Glucose utilization via glycogen phosphorylase sustains proliferation and prevents premature senescence in cancer cells. *Cell metabolism* **2012**, *16*, 751−764.
(39) Philips, K. B.; et al. Increased sensitivity to glucose starvation correlates with downregulation of glycogen phosphorylase isoform PYGB in tumor cell lines resistant to 2-deoxy-D-glucose. *Cancer chemotherapy and pharmacology* **2014**, *73*, 349−361.
(40) Zhou, Y.; Jin, Z.; Wang, C. Glycogen phosphorylase B promotes ovarian cancer progression via Wnt/β-catenin signaling and is regulated by miR-133a-3p. *Biomedicine & Pharmacotherapy* **2019**, *120*, No. 109449.
(41) de Luna, N.; et al. Sodium valproate increases the brain isoform of glycogen phosphorylase: looking for a compensation mechanism in McArdle disease using a mouse primary skeletal-muscle culture in vitro. *Disease models & mechanisms* **2015**, *8*, 467−472.
(42) Han, S.; et al. MicroRNA-1251−5p promotes tumor growth and metastasis of hepatocellular carcinoma by targeting AKAP12. *Biomed Pharmacother* **2020**, *122*, No. 109754.
(43) Jewell, M. L.; et al. Single-Cell RNA Sequencing Identifies Yes-Associated Protein 1-Dependent Hepatic Mesothelial Progenitors in Fibrolamellar Carcinoma. *Am. J. Pathol.* **2020**, *190*, 93−107.
(44) Steinauer, N.; Guo, C.; Zhang, J. Emerging Roles of MTG16 in Cell-Fate Control of Hematopoietic Stem Cells and Cancer. *Stem Cells Int.* **2017**, *2017*, No. 6301385.
(45) Thirant, C.; et al. ETO2-GLIS2 Hijacks Transcriptional Complexes to Drive Cellular Identity and Self-Renewal in Pediatric Acute Megakaryoblastic Leukemia. *Cancer Cell* **2017**, *31*, 452−465.
(46) Boxberger, K. H.; Hagenbuch, B.; Lampe, J. N. Common drugs inhibit human organic cation transporter 1 (OCT1)-mediated neurotransmitter uptake. *Drug Metab. Dispos.* **2014**, *42*, 990−995.
(47) Soto, M.; et al. Relationship between changes in the exon-recognition machinery and SLC22A1 alternative splicing in hepatocellular carcinoma. *Biochimica et Biophysica Acta (BBA) - Molecular Basis of Disease* **2020**, *1866*, No. 165687.
(48) Herraez, E.; et al. Expression of SLC22A1 variants may affect the response of hepatocellular carcinoma and cholangiocarcinoma to sorafenib. *Hepatology* **2013**, *58*, 1065−1073.
(49) Chen, X.; Xia, Z.; Wan, Y.; Huang, P. Identification of hub genes and candidate drugs in hepatocellular carcinoma by integrated bioinformatics analysis. *Medicine (Baltimore)* **2021**, *100*, No. e27117.
(50) Savage, D. G.; Antman, K. H. Imatinib mesylate−a new oral targeted therapy. *N Engl J. Med.* **2002**, *346*, 683−693.
(51) Kolibaba, K. S.; Druker, B. J. Protein tyrosine kinases and cancer. *Biochim. Biophys. Acta* **1997**, *1333*, F217−248.
(52) Cervello, M.; et al. Molecular mechanisms of sorafenib action in liver cancer cells. *Cell cycle (Georgetown, Tex.)* **2012**, *11*, 2843−2855.
(53) Bruix, J.; et al. Efficacy and safety of sorafenib in patients with advanced hepatocellular carcinoma: subanalyses of a phase III trial. *Journal of hepatology* **2012**, *57*, 821−829.
(54) Zhou, J.; Goh, B.-C.; Albert, D. H.; Chen, C.-S. ABT-869, a promising multi-targeted tyrosine kinase inhibitor: from bench to bedside. *J. Hematol. Oncol.* **2009**, *2*, 33.
(55) Toh, H. C.; et al. Phase 2 trial of linifanib (ABT-869) in patients with unresectable or metastatic hepatocellular carcinoma. *Cancer* **2013**, *119*, 380−387.
(56) Hirose, Y.; et al. Inhibition of Stabilin-2 elevates circulating hyaluronic acid levels and prevents tumor metastasis. *Proc. Natl. Acad. Sci. U. S. A.* **2012**, *109*, 4263−4268.
(57) Han, M. W.; et al. Homotypic Interaction of Stabilin-2 Plays a Critical Role in Lymph Node Metastasis of Tongue Cancer. *Anticancer Res.* **2016**, *36*, 6611−6618.
(58) Miller, C. M.; et al. Stabilin-1 and Stabilin-2 are specific receptors for the cellular internalization of phosphorothioate-modified antisense oligonucleotides (ASOs) in the liver. *Nucleic Acids Res.* **2016**, *44*, 2782−2794.
(59) Dhar, D.; Antonucci, L.; Nakagawa, H.; Kim, J. Y.; Glitzner, E.; Caruso, S.; Shalapour, S.; Yang, L.; Valasek, M. A.; Lee, S.; et al. Liver Cancer Initiation Requires p53 Inhibition by CD44-Enhanced Growth Factor Signaling. *Cancer Cell* **2018**, *33*, 1061−1077.e6.

https://doi.org/10.1021/acsomega.4c01496
ACS Omega 2024, 9, 26075−26096

(60) Lee, K. H. CaMKII Inhibitor KN-62 Blunts Tumor Response to Hypoxia by Inhibiting HIF-1α in Hepatoma Cells. *Korean J. Physiol Pharmacol* **2010**, *14*, 331−336.
(61) Hudmon, A.; Schulman, H. Structure-function of the multifunctional Ca^{2+}/calmodulin-dependent protein kinase II. *Biochem. J.* **2002**, *364*, 593−611.
(62) Xia, W.; et al. MiR-103 regulates hepatocellular carcinoma growth by targeting AKAP12. *international journal of biochemistry & cell biology* **2016**, *71*, 1−11.

https://doi.org/10.1021/acsomega.4c01496
ACS Omega 2024, 9, 26075−26096